PREDICTION OF TWO-PHASE PERFORMANCE OF CENTRIFUGAL PUMPS

Albert Louis Goldfinch

PREDICTION OF TWO-PHASE PERFORMANCE OF CENTRIFUGAL PUMPS

by

ALBERT LOUIS GOLDFINCH, SR.

B.E., Vanderbilt University
(1968)

Submitted in Partial Fulfillment of the Requirements

for the Degree of

OCEAN ENGINEER

and the Degree of

MASTER OF SCIENCE IN MECHANICAL ENGINEERING

at the

MASSACHUSETTS INSTITUTE OF TECHNOLOGY

May, 1976

PREDICTION OF TWO-PHASE PERFORMANCE
OF CENTRIFUGAL PUMPS

by

ALBERT LOUIS GOLDFINCH, SR.

Submitted to the Department of Ocean Engineering on 7 May 1976, in partial fulfillment of the requirements for the degree of Ocean Engineer and the degree of Master of Science in Mechanical Engineering.

ABSTRACT

Safety analyses of a loss-of-coolant accident in a pressurized-water-reactor nuclear power plant require modeling the flow through the main-coolant pumps in any one of several extreme operating conditions. A semi-empirical method of predicting the two-phase performance of centrifugal pumps has been proposed and was applied to normal pump operation with good results. In this report the proposed method is applied to the reverse-flow, reverse-rotation mode of operation, also with good results.

By making simplifying assumptions, the flow through the pump is idealized and expressions for the theoretical pump characteristics derived from Euler's equation for the mean flow through a turbomachine. General expressions for the flow losses in two-phase flow are derived, and the flow losses expressed as the difference between the theoretical characteristics and the actual performance of the pump. The ratio of the losses in two-phase flow to those in single-phase flow is shown to be primarily a function of pump geometry and fluid void-fraction. Using experimental data from single- and two-phase flow tests on a pump of known geometry, the ratio of the losses was calculated for various conditions of flow and plotted as a function of void fraction. The results plotted in this fashion show excellent correlation and the function can be used to predict the two-phase characteristics of similar pumps.

Thesis Supervisor: David Gordon Wilson
Title: Professor of Mechanical Engineering

Thesis Reader: A. Douglas Carmichael
Title: Professor of Power Engineering

ACKNOWLEDGEMENTS

I would like to express my thanks to Professor David Gordon Wilson for his encouragement and guidance in this project. I also wish to thank Mr. Tak-chee Chan, Mr. Ray Zegley and Professor Peter Griffith for their advice and suggestions, and Mrs. Sandy Margeson for being able to type so expertly from my handwriting.

Above all, thanks to Lib, Nancy, Albert Jr., and Charlene.

TABLE OF CONTENTS

LIST OF SYMBOLS

A	flow area
a	two-phase flow function $\equiv \left[\frac{\alpha}{1-\alpha}\right] \frac{\rho_v}{\rho_L}$
c	fluid velocity, absolute
f_{tp}	two-phase flow function (eq. 8a)
g	gravitational acceleration
g_c	constant in Newton's Law
H	head
H^*	head-loss ratio $\equiv \frac{\Delta H_{otpth} - \Delta H_{otp}}{\Delta H_{ospth} - \Delta H_{osp}}$
h	enthalpy
K, K_4, K_5, K_6	constants defined by eqs. 12, 13, and 15
$\dot{m}$	mass flow per unit time
N	rotor speed, rev/min
p	fluid pressure
Q	volume flow per unit time
r	impeller radius
R	friction-factor multiplier $\equiv \left[\frac{1-x}{1-\alpha}\right]^2$
s	slip velocity ratio $\equiv (C_v/C_L)$
U	rotor peripheral velocity
w	fluid velocity relative to rotor
x	quality $\equiv (\dot{m}_v/\dot{m}_T)$
α	void fraction $\equiv (A_v/A_T)$
β	angle of fluid vector relative to tangent to rotor periphery
β'	angle of tangent to rotor-blade centerline relative to tangent to rotor periphery

Δ	property difference
δ	deviation angle
ε	flow ratio $\equiv (Q_{be}/Q_{tp})$
ρ	fluid density
ϕ	flow coefficient $\equiv (C_m/U)$
ψ	work coefficient $\equiv (g_c \Delta h_o/U^2)$
ψ'	head coefficient $\equiv (g\Delta H_o/U^2)$

SUBSCRIPTS

o	total (static plus dynamic) or stagnation value of property
1	plane at entrance to rotor
2	plane at exit from rotor
3	plane at entrance to pump
be	best-efficiency point
f	wall-friction component
L	liquid
m	meridional or radial component of velocity
θ	tangential component of velocity
s	flow-separation component
sp	single-phase component
T	total flow, liquid plus vapor
tp	two-phase flow
th	theoretical or ideal conditions
v	vapor

INTRODUCTION

BACKGROUND

In a nuclear power plant of the pressurized-water-reactor type (PWR), sub-cooled water at high pressure and temperature is circulated through the reactor core by several main-coolant pumps, each in its own coolant leg. Safety analyses of postulated loss of coolant accidents (LOCA) require models of the flow through the main-coolant pumps for any one of several operating modes in both single- and two-phase flow. In an effort to more precisely predict the contribution of the main-coolant pumps to flow through the reactor core during a LOCA, there has been a continuing effort to improve these models, particularly for two-phase flow.

A semi-empirical method for predicting the two-phase flow performance of a centrifugal pump was proposed by Mikielewicz and Wilson,[1] and was applied to normal pump operation (forward rotation and flow) with promising results. Details of their procedure are summarized below.

Starting with the Euler equation a theoretically-ideal head-versus-flow relationship is derived for both single- and two-phase flow.

By examining the hydraulic losses in two-phase flow it is shown that for a given pump the relative pressure losses--the difference between theoretical

and actual pressure rise--are related to the relative pressure losses in single-phase flow by a function of void fraction, a property of the two-phase fluid.

The ratio of relative pressure losses in two-phase flow to those in single-phase flow is defined as the "Head-loss ratio".

The head-loss ratio is then calculated by combining the derived theoretical characteristics with experimental data for single- and two-phase flow.

For first quadrant operation, good correlation is shown between the head-loss ratio and void fraction, and the result can be used to predict the two-phase characteristics of the pump.

It is shown that the head-loss ratio for a given pump is related to other pumps by a function of pump geometry; further experimental work is required to determine this relationship.

PURPOSE

The purpose of this report is to determine if the procedure is applicable to the third quadrant of operation (reverse-flow and rotation). The steps of the procedure, as outlined, will be modified only as required by the different flow geometry, and the terminology used will be the same.

PROCEDURE

DERIVATION OF THEORETICAL CHARACTERISTICS

A centrifugal pump subjected to conditions such that its normal flow and rotation directions are reversed will operate in a manner similar to a radial-in-flow turbine. The Euler equation can be applied to determine the characteristics of the pump in this mode of operation:

$$g_c \ \Delta h_o = U_1 C_{\theta 1} - U_2 C_{\theta 2} \qquad (1)$$

where:

$C_\theta \equiv$ fluid tangential velocity

$g_c \equiv$ constant in Newton's Law

$\Delta h_o \equiv$ change in total enthalpy = $h_{o1} - h_{o2}$

$U \equiv$ rotor peripheral velocity

subscript 1 $\equiv$ rotor entrance

subscript 2 $\equiv$ rotor outlet

The fluid tangential velocity at rotor outlet, $C_{\theta 2}$, could be significant because conditions of flow and rotor speed would be other than optimum and because, in general, a pump is not designed to be an efficient turbine. For these reasons the simplifying assumption of zero outlet swirl will not be made. This general form of the equation

is exact and will yield the actual enthalpy change across the pump, for any flow condition, if the proper values for the velocities are used.

In the inlet region of the pump, Figure 1, precise flow angles and velocities are unknown and an assumption must be made relating $C_{\theta 1}$ to the flow rate entering the scroll. Using this assumed value of $C_{\theta 1}$ the velocity triangle at the rotor entrance, as shown in Figure 2, can be solved for all velocities in terms of the flow rate.

At the rotor outlet, flow geometry is specified by the design of what is normally the impeller inlet eye. A typical design with swept-back blading is shown in Figure 3. Reverse flow and rotation will produce a velocity diagram as shown in Figure 4, which can also be solved for all velocities in terms of the flow rate.

If the reverse flow through the pump is idealized by making simplifying assumptions, the Euler equation can be used to approximate the theoretical head and flow characteristics of the pump. The following flow conditions are assumed.

1. That the fluid tangential velocity at rotor entrance, $C_{\theta 1}$, is equal in magnitude to the absolute fluid velocity, C_3, entering the scroll.
2. That the relative flow angle at rotor outlet, β_2, is constant for all flow rates and conditions.
3. That the deviation angle at rotor outlet, δ_2, is zero, that is, $\beta_2' = \beta_2$.

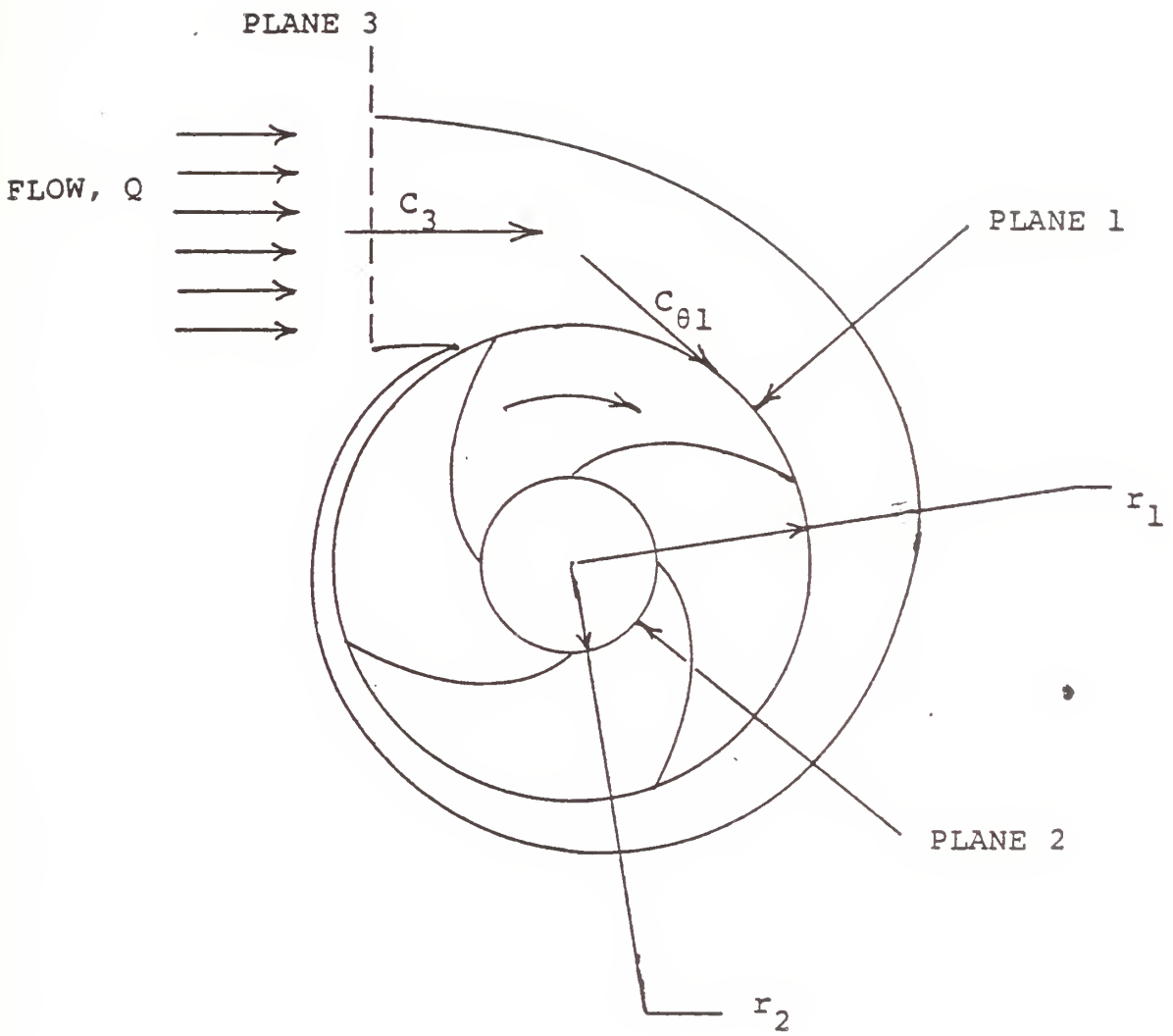

FIGURE 1 - TYPICAL CENTRIFUGAL PUMP IN REVERSE-FLOW AND ROTATION

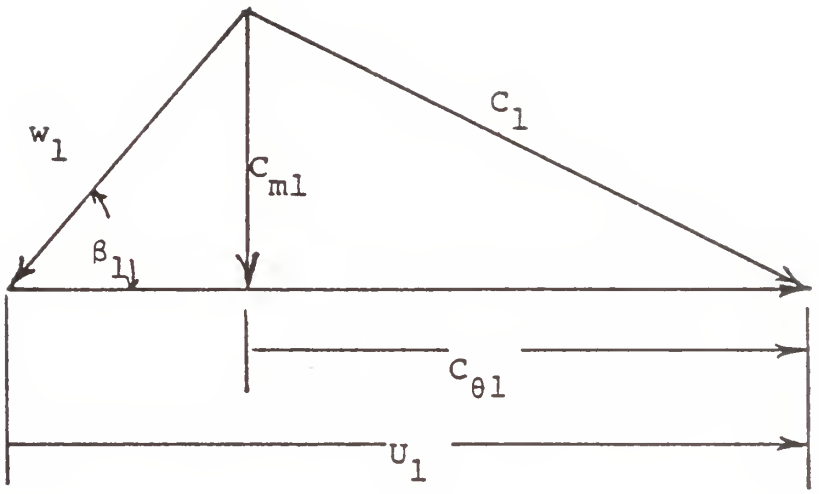

U_1 - rotor peripheral velocity

C_1 - fluid absolute velocity

$C_{\theta 1}$ - fluid tangential velocity

C_{m1} - fluid radial velocity

w_1 - fluid relative velocity

β_1 - fluid relative flow angle

FIGURE 2 - VELOCITY DIAGRAM AT IMPELLER INLET

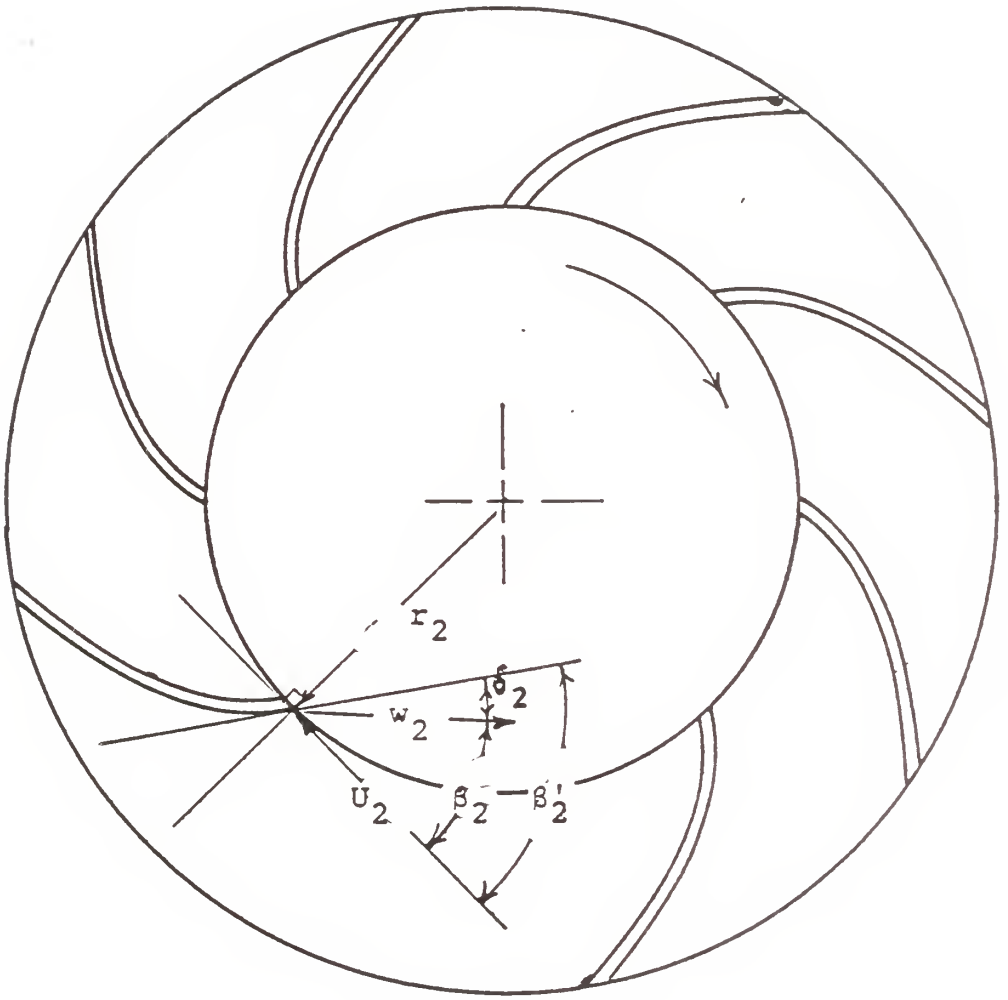

FIGURE 3 - TYPICAL IMPELLER-EYE WITH REVERSE-FLOW AND ROTATION

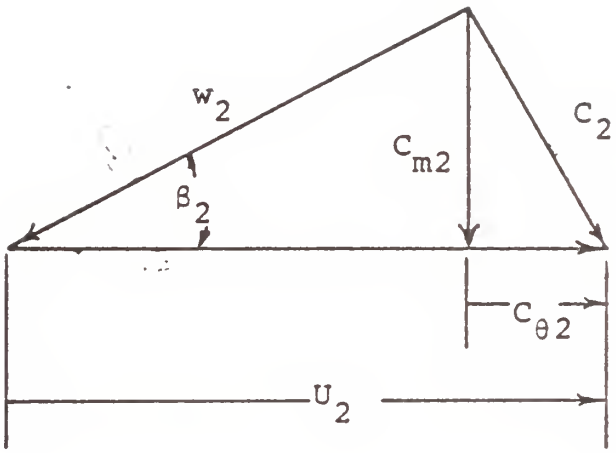

FIGURE 4 - VELOCITY DIAGRAM AT IMPELLER OUTLET

With the above assumptions, equation 1 becomes

$$g_c \Delta h_{o\,th} = U_1 C_{\theta 1} - U_2 C_{\theta 2} \qquad (2)$$

where

subscript th ≡ theoretical or ideal conditions

For the specific case of loss-less incompressible flow, the theoretical total enthalpy change is proportional to the change in theoretical total head.[1]

$$g_c \Delta h_{o\,th} = g \Delta H_{o\,th}$$

where

ΔH_o ≡ change in total head = $H_{o1} - H_{o2}$

g ≡ gravitational acceleration

and the expression for the theoretical total head characteristics of the pump is:

$$g \Delta H_{oth} = U_1 C_{\theta 1} - U_2 C_{\theta 2} \qquad (3)$$

Theoretical single-phase-flow characteristics

For single-phase flow, the velocity triangles are solved by using the continuity equation and the assumptions made to idealize the flow.

In the pump inlet region, it was assumed that

$$C_{\theta 1} = C_3$$

where

subscript 3 ≡ plane at inlet to pump

From continuity

$$Q = C_3 A_3 = C_{m1} A_1$$

where

Q ≡ volume flow per unit time

A ≡ area normal to the flow

subscript m ≡ meridional or radial component of velocity

therefore,

$$C_{\theta 1} = C_{m1} \frac{A_1}{A_3} \tag{4}$$

At the rotor outlet, from Figure 4,

$$C_{\theta 2} = U_2 - \frac{C_{m2}}{\tan \beta_2}$$

Since

$$U_2 = U_1 \frac{r_2}{r_1}$$

where

$\frac{r_2}{r_1}$ = rotor-outlet-to-inlet radius-ratio

and by continuity

$$C_{m2} = C_{m1} \frac{A_1}{A_2}$$

then,

$$C_{\theta 2} = U_1 \frac{r_2}{r_1} - \frac{A_1}{A_2} \frac{C_{m1}}{\tan \beta_2} \qquad (5)$$

By substituting equations 4 and 5, equation 3 becomes

$$g \Delta H_{othsp} = U_1 C_{m1} \frac{A_1}{A_3} - U_1 \frac{r_2}{r_1}\left[U_1 \frac{r_2}{r_1} - \frac{A_1}{A_2} \frac{C_{m1}}{\tan \beta_2}\right]$$

where

subscript sp ≡ single-phase flow

Dividing by U_1^2 and defining the head coefficient, ψ_1', as

$$\psi_1' \equiv \frac{g\Delta H_o}{U_1^2}$$

and the flow coefficient, ϕ_1, as

$$\phi_1 \equiv \frac{C_{m1}}{U_1}$$

equation 3 becomes

$$\psi'_{1thsp} = -\left(\frac{r_2}{r_1}\right)^2 + \left[\frac{A_1}{A_3} + \frac{r_2}{r_1}\,\frac{A_1}{A_2 \tan \beta_2}\right] \phi_1 \qquad (6)$$

This expression is a linear function of ψ' versus ϕ, and is similar to the expression derived for first-quadrant operation.

Theoretical two-phase-flow characteristics

In two-phase separated flow it is assumed that the liquid and the vapor phases have separate mass flows and that their velocity components may also be different. In this case, equation 2 becomes

$$\psi'_{1thtp} = \frac{1}{U_1}[(1-x_1)C_{\theta L1}+x_1 C_{\theta v1}] - \frac{U_2}{U_1^2}[(1-x_2)C_{\theta L2}+x_2 C_{\theta v2}]$$

where

$x \equiv$ quality $\equiv \dot{m}_v/\dot{m}_L$

and $\dot{m} \equiv$ mass flow per unit time

subscripts L $\equiv$ liquid

T $\equiv$ total flow, liquid + vapor

tp $\equiv$ two-phase flow

v $\equiv$ vapor

From the velocity triangles at rotor inlet and outlet and from the assumption that $C_{\theta 1} = C_3$,

$$\psi'_{1thtp} = \frac{1}{U_1}\left[(1-x_1)C_{mL1}\frac{A_1}{A_3} + x_1 C_{mv1}\frac{A_1}{A_3}\right] - \frac{U_2^2}{U_1^2}\left[(1-x_2)\left(1-\frac{C_{mL2}}{U_2 \tan \beta_2}\right)+x_2\left(1-\frac{C_{mv2}}{U_2 \tan \beta_2}\right)\right]$$

From continuity

$$C_{mL} = \frac{\dot{m}_L}{\rho_L A_L} = \frac{\dot{m}_T (1-x)}{\rho_L (1-\alpha) A_T}$$

$$C_{mv} = \frac{\dot{m}_v}{\rho_v A_v} = \frac{\dot{m}_T x}{\rho_v \alpha A_T}$$

where

$\alpha \equiv$ void fraction $\left(\frac{A_v}{A_T}\right)$

$\rho \equiv$ fluid density

and by defining the two-phase-flow coefficient, ϕ_{tp}, as

$$\phi_{tp} \equiv \frac{Q_{tp}}{A\ U} = \frac{\dot{m}_T}{\rho_{tp}\ A\ U}$$

where

$\rho_{tp} \equiv$ mean density of two-phase flow

$$= (1-\alpha)\rho_L + \alpha\rho_v$$

Equation 2 becomes

$$\psi'_{1thtp} = \frac{A_1}{A_3}\phi_{tp1}\left[(1-x_1)^2 + (1-x_1)^2 \frac{\alpha_1}{(1-\alpha_1)} \frac{\rho_{v1}}{\rho_{L1}} + x_1^2 \frac{(1-\alpha_1)}{\alpha_1} \frac{\rho_{L1}}{\rho_{v1}} + x_1^2\right] - \frac{U_2^2}{U_1^2}\left\{1 - \frac{\phi_{tp2}}{\tan \beta_2}\left[1 + \frac{\alpha_2}{(1-\alpha_2)} \frac{\rho_{v2}}{\rho_{L2}}\right]\right.$$

$$\left.\left[(1-x_2)^2 + \frac{(1-\alpha_2)}{\alpha_2} \frac{\rho_{L2}}{\rho_{v2}} x_2^2\right]\right\} \qquad (7)$$

By defining a two-phase-flow function, a,

$$a \equiv \left(\frac{\alpha}{1-\alpha}\right) \frac{\rho_v}{\rho_L}$$

and a two-phase slip-velocity ratio, s,

$$s \equiv \frac{C_v}{C_L}$$

The quality of the fluid can be expressed as

$$x = \frac{as}{1+as}$$

By substituting these expressions, equation 7 becomes

$$\psi'_{1thtp} = \frac{A_1}{A_3}\,\phi_{tp1}\,\frac{(1+a_1)(1+a_1 s_1^2)}{(1+a_1 s_1)^2} - \left(\frac{r_2}{r_1}\right)^2 \left[1-\frac{\phi_{tp2}}{\tan\beta_2}\,\frac{(1+a_2)(1+a_2 s_2^2)}{(1+a_2 s_2)^2}\right] \tag{8}$$

Applying the continuity equation to the two-phase flow coefficients at rotor inlet and outlet yields,

$$\phi_{tp2} = \phi_{tp1}\,\frac{\rho_{tp1}}{\rho_{tp2}}\,\frac{A_1}{A_2}\,\frac{U_1}{U_2}$$

which reduces equation 8 to

$$\psi'_{1thtp} = \frac{A_1}{A_3}\,\phi_{tp1}\,f_{tp1} - \left(\frac{r_2}{r_1}\right)^2 \left[1-\frac{\phi_{tp1}}{\tan\beta_2}\,f_{tp2}\,\frac{\rho_{tp1}}{\rho_{tp2}}\,\frac{A_1}{A_2}\,\frac{U_1}{U_2}\right]$$

where

$$f_{tp} \equiv \frac{(1+a)(1+as^2)}{(1+as)^2} \tag{8a}$$

Rearranging:

$$\psi'_{1thtp} = -\left(\frac{r_2}{r_1}\right)^2 + \left[\frac{A_1}{A_3} f_{tp1} + \frac{r_2}{r_1} \frac{\rho_{tp1}}{\rho_{tp2}} \frac{A_1}{A_2} \frac{f_{tp2}}{\tan \beta_2}\right] \phi_{tp1} \tag{9}$$

If the flow becomes single-phase, equation 9 reduces to the single-phase case, equation 6, because f_{tp1}, f_{tp2} and ρ_{tp1}/ρ_{tp2} all equal unity when the void fraction, α, equals zero.

As derived, equation 9 is cumbersome and requires a knowledge of the relationships between inlet and outlet conditions to calculate values of the head coefficient for various conditions of void fraction and flow. By assuming that fluid properties at rotor inlet and outlet are equal, equation 9 reduces to

$$\psi'_{1thtp} = -\left(\frac{r_2}{r_1}\right)^2 + \left[\frac{A_1}{A_3} + \frac{r_2}{r_1} \frac{A_1}{A_2 \tan \beta_2}\right] f_{tp1} \phi_{tp1} \tag{10}$$

The assumption is valid in this case because the moment of momentum at rotor outlet, $U_2 C_{\theta 2}$, is very small in comparison to $U_1 C_{\theta 1}$, and the outlet properties appear in the term derived from $U_2 C_{\theta 2}$; thus the effect of changes in fluid properties from inlet to outlet is minimal.

The two-phase flow function, f_{tp}, was defined by equation 8a as

$$f_{tp} \equiv \frac{(1+a)(1+as^2)}{(1+as)^2}$$

where

$$a \equiv \left(\frac{\alpha}{1-\alpha}\right) \frac{\rho_v}{\rho_L}$$

$$s \equiv \frac{C_v}{C_L}$$

For a steam-water mixture, liquid and vapor densities are given by steam tables for various pressures. The slip-velocity ratio, s, for two-phase flow in a horizontal pipe, was correlated as a function of pressure and void fraction[2] as shown in Figure 5. A correlation more applicable to two-phase flow in centrifugal pumps was not available; therefore, the relationship described, though for vastly different conditions of flow, was applied.

Values of the two-phase flow function, f_{tp}, can be calculated as a function of void fraction, α, for various pressures, as shown in Figure 6.

The theoretical characteristics for third-quadrant operation of a centrifugal pump in both single- and two-phase flow can be represented as shown in Figure 7. In single-phase flow, f_{tp} is unity; in two-phase flow, f_{tp} is determined by pressure and void fraction.

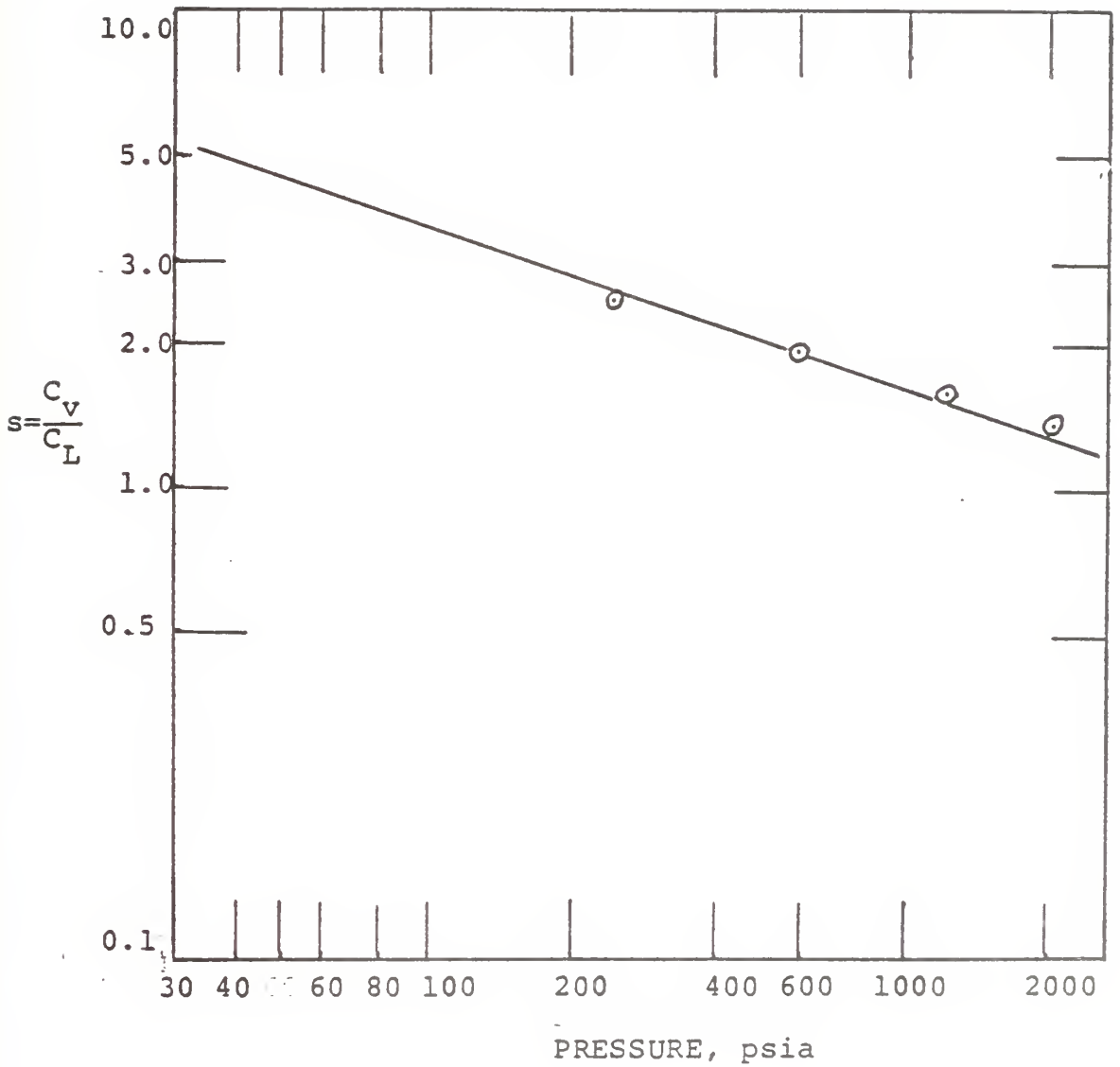

FIGURE 5 - SLIP-VELOCITY RATIO, s, VERSUS PRESSURE

(from reference 2)

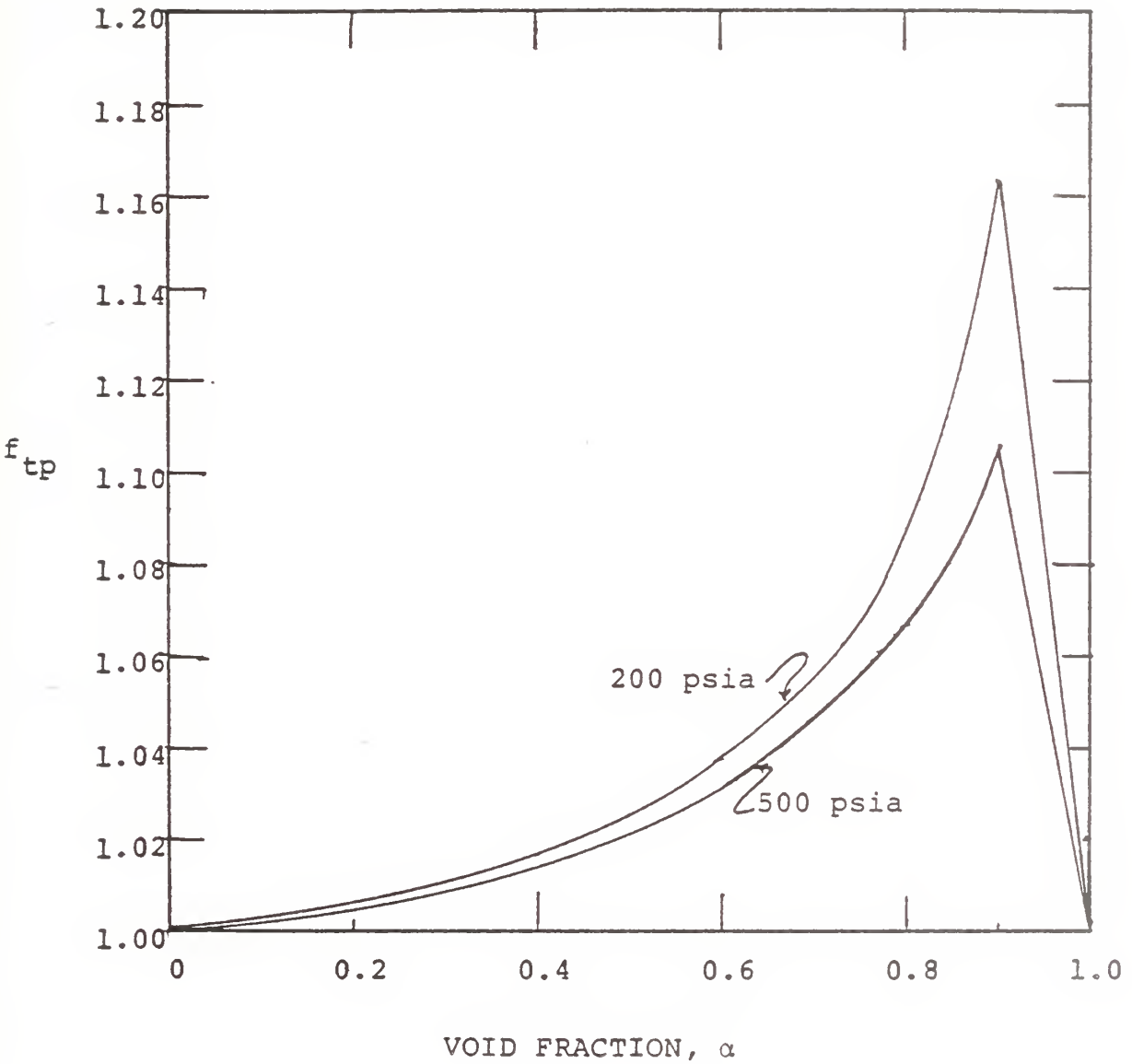

FIGURE 6 - TWO-PHASE FLOW FUNCTION, f_{tp}, VERSUS VOID FRACTION, α, FOR 200 AND 500 psia

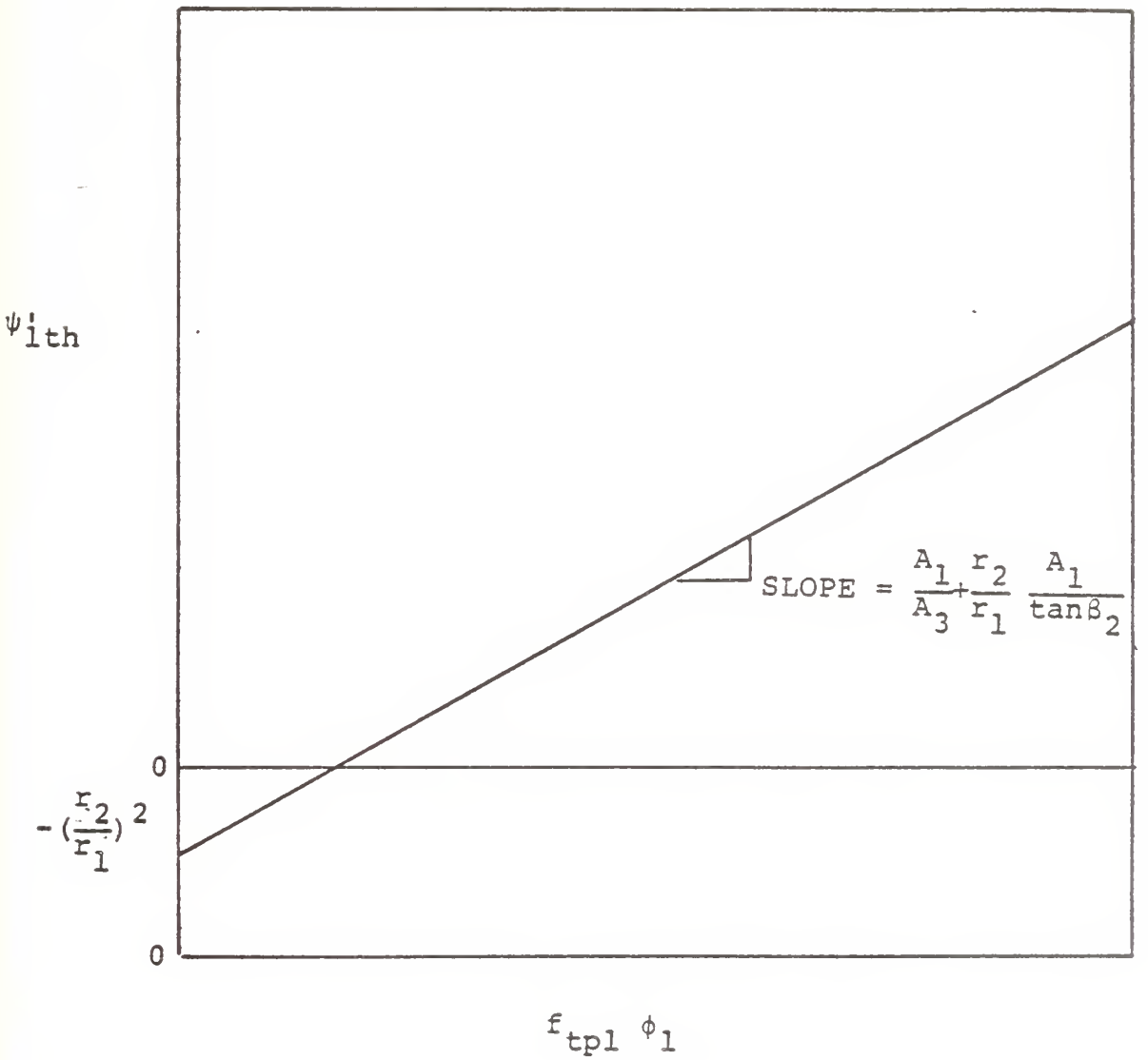

FIGURE 7 - THEORETICAL HEAD-VERSUS-FLOW CHARACTERISTICS

FLOW LOSSES

At a given rate of flow through a centrifugal pump, the difference between the measured head and the theoretically ideal head is the result of flow losses generated within the pump, and changes in the exit deviation angle, δ_2, from the assumed ideal direction. For third-quadrant operation, in single-phase flow, this difference is shown in Figure 8. The curve of actual head versus flow is typical for this quadrant,[3,4] and the theoretical relationship is approximated from the previously derived expression (equation 6).

The actual head, ΔH_o, is a function of the flow-rate, Q, squared;[3] therefore, with flow increasing from zero, the losses decrease as the square of the flow, pass through a minimum, then increase as the square of the flow. The flow-rate corresponding to the point of minimum losses is defined as the best efficiency flow, Q_{be}, for third-quadrant operation.

In the first-quadrant of operation, the flow losses behave in a similar manner and the expressions derived to relate the losses in two-phase flow to the losses in single-phase flow may be applied to the third-quadrant. The constants and flow-rate ratio are those applicable to the third quadrant.

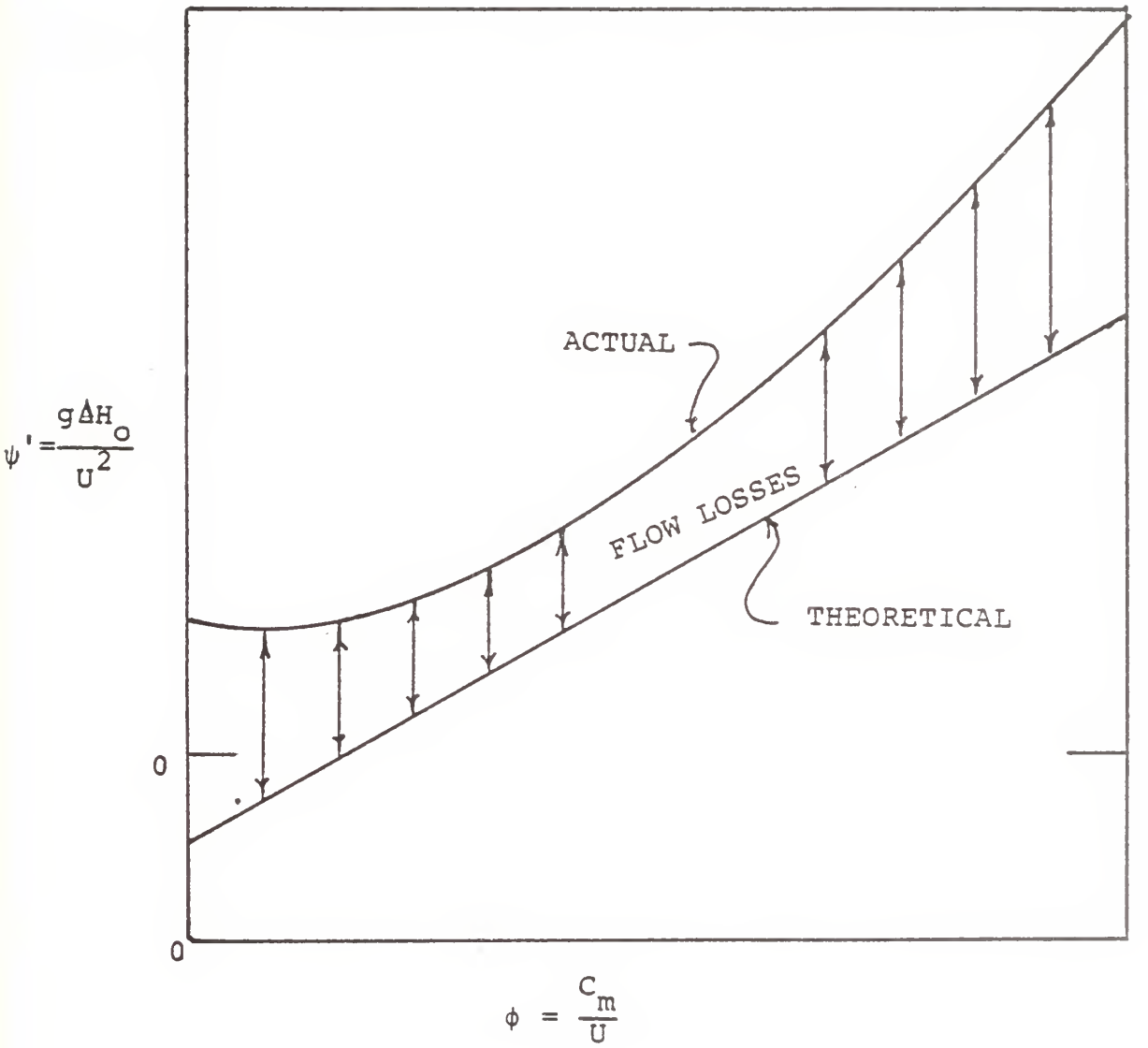

FIGURE 8 - TYPICAL THEORETICAL AND ACTUAL PUMP CHARACTERISTICS

The flow losses are expressed as the sum of wall-friction losses and flow-separation losses,

$$\Delta p_o = \Delta p_{of} + \Delta p_{os} \tag{11}$$

where

$\Delta p_o \equiv$ loss of total, or stagnation, pressure

subscripts f ≡ friction component

s ≡ flow-separation component

The wall-friction component of the losses in two-phase flow is given by

$$\Delta p_{otpf} = R\ K\ \left(\frac{\rho_{tp}}{\rho_L}\right)^2\ Q_{tp}^2 \tag{12}$$

where

$R \equiv$ friction factor multiplier[5] $\left[\frac{1-x}{1-\alpha}\right]^2$

$K \equiv$ constant at high Reynolds' numbers; includes pump geometry, the single-phase friction factor, and liquid density

By approximating the flow-separation losses as proportional to the square of the difference between the existing flow and the flow at best efficiency point,[6] Q_{be}, the two-phase flow-separation losses become

$$\Delta p_{otps} = K_4 \, Q_{tp}^2 \, [(1-\alpha)(\frac{1+a}{1+sa}) - \varepsilon]^2 \qquad (13)$$

where

$K_4 \equiv$ constant, depends on flow regime

$\varepsilon \equiv Q_{be}/Q_{tp}$

Adding these components yields the expression for the total losses in two-phase flow, Δp_{otp},

$$\Delta p_{otp} = R \, K \, (\frac{\rho_{tp}}{\rho_L})^2 \, Q_{tp}^2 + K_4 \, Q_{tp}^2 [(1-\alpha)(\frac{1+a}{1+sa}) - \varepsilon]^2 \qquad (14)$$

substituting

$$\frac{\rho_{tp}}{\rho_L} = [\frac{1-\alpha}{1-x}][\frac{1+a}{1+sa}]$$

The total losses in two-phase flow become

$$\Delta p_{otp} = K_5\{(\frac{1+a}{1+sa})^2 + K_6[(1-\alpha)(\frac{1+a}{1+sa})-\varepsilon]^2\} \, Q_{tp}^2 \qquad (15)$$

where

K_5 and K_6 are constants which include geometric and flow-regime factors

for single-phase flow, equation 15 reduces to

$$\Delta p_{osp} = K_5[1 + K_6(1-\varepsilon)^2] \, Q_L^2 \qquad (16)$$

The comparison between single-phase and two-phase flow is made at like values of flow-rate; therefore, the ratio of two-phase to single-phase losses is

$$\frac{\Delta p_{otp}}{\Delta p_{osp}} = \frac{\left(\frac{1+a}{1+sa}\right)^2 + K_6\left[(1-\alpha)\left(\frac{1+a}{1+sa}\right) - \varepsilon\right]^2}{1 + K_6(1-\varepsilon)^2} \qquad (17)$$

HEAD-LOSS RATIO

The total losses, Δp_o, can be expressed as the difference between the actual and the theoretical heads at a given flow-rate,

$$\Delta p_o = (\Delta H_o - \Delta H_{oth})\ \rho\frac{g}{g_c} \qquad (18)$$

In terms of head, equation 17 becomes

$$\frac{\Delta H_{otp} - \Delta H_{othtp}}{\Delta H_{osp} - \Delta H_{othsp}} = \frac{\rho_L}{\rho_{tp}} \quad \frac{\left(\frac{1+a}{1+sa}\right)^2 + K_6\left[(1-\alpha)\left(\frac{1+a}{1+sa}\right) - \varepsilon\right]^2}{1+K_6(1-\varepsilon)^2} \qquad (19)$$

substituting

$$\frac{\rho_L}{\rho_{tp}} = \left(\frac{1-x}{1-\alpha}\right)\left(\frac{1+a}{1+sa}\right)$$

and $x = \frac{sa}{1+sa}$

Equation 19 becomes

$$\frac{\Delta H_{otp} - \Delta H_{othtp}}{\Delta H_{osp} - \Delta H_{othsp}} = \frac{\left(\frac{1+a}{1+sa}\right)^2 + K_6\left[(1-\alpha)\left(\frac{1+a}{1+sa}\right)-\varepsilon\right]^2}{(1-\alpha)(1+a)\left[1+K_6(1-\varepsilon)^2\right]} \qquad (20)$$

For the first quadrant, the head-loss ratio, H*, was defined as

$$H^* \equiv \frac{\Delta H_{othtp} - \Delta H_{otp}}{\Delta H_{othsp} - \Delta H_{osp}}$$

To prevent the introduction of an unnecessary change, the first quadrant definition will be used in the third quadrant as it is numerically equal to the ratio in equation 20. Thus, for third quadrant operation

$$H^* = \frac{\Delta H_{othtp} - \Delta H_{otp}}{\Delta H_{othsp} - \Delta H_{osp}} = f\left[\left(\frac{1+a}{1+sa}\right), \alpha, K_6, \varepsilon\right] \qquad (21)$$

In this functional relationship: (1+a/1+sa) is a function of void fraction and pressure; K_6 includes the geometry of a given pump and the flow regime of the two-phase fluid (a function of void fraction); and ε is the ratio of best efficiency flow in third-quadrant operation to the existing flow. For a given pump, operating at a particular pressure, the ratio of two-phase to single-phase losses at like values of ε is therefore principally a function of the void fraction of the two-phase fluid.

Substituting the definition for the head coefficient, ψ',

$$\psi' \equiv \frac{g\Delta H_o}{U^2}$$

the head-loss ratio can be expressed as

$$H^* = \frac{\psi'_{thtp} - \psi'_{tp}}{\psi'_{thsp} - \psi'_{sp}} \tag{22}$$

CALCULATION OF THE HEAD-LOSS RATIO

The head-loss ratio as a function of void fraction for third-quadrant operation of a particular centrifugal pump can be constructed using the derived theoretical characteristics and the actual characteristics obtained from experimental data. The relationship between H* and α for this pump can then be used to predict the third-quadrant, two-phase performance of other pumps as single-phase characteristics are usually known or can be easily determined.

D.J. Olson conducted experiments on a semi-scale pump of known geometry,[7] in single- and two-phase flow, and in the operating quadrants of interest. Using the results of his experiments in the third quadrant, the actual characteristics of the pump can be calculated. Information obtained from the pump manufacturer[8] provided the required constants for calculation of the theoretical characteristics for the pump using equation 10.

The functional relationship between head-loss ratio and void fraction for this particular pump is developed as described in the following sections. Details of Olson's apparatus and test conditions are shown in Appendix D.

Theoretical head-coefficients

Details of the semi-scale pump used by Olson are shown in Figures 9 and 10. With proper values substituted for the constants, equation 10 becomes

$$\psi'_{lth} = -0.1896 + 9.155\ f_{tpl}\ \phi_l$$

As previously described, this equation may be used to determine the theoretical characteristics in both single- and two-phase flow.

Actual single-phase head-coefficient

A non-dimensional head-flow curve for the semi-scale pump can be constructed, as shown in Figure 11, using the single-phase data. Curve-fitting the points by regression, using the method of least squares, this curve is accurately approximated by the expression

$$\psi'_{lsp} = 101.28\ \phi_l^{1.8756} + 0.4$$

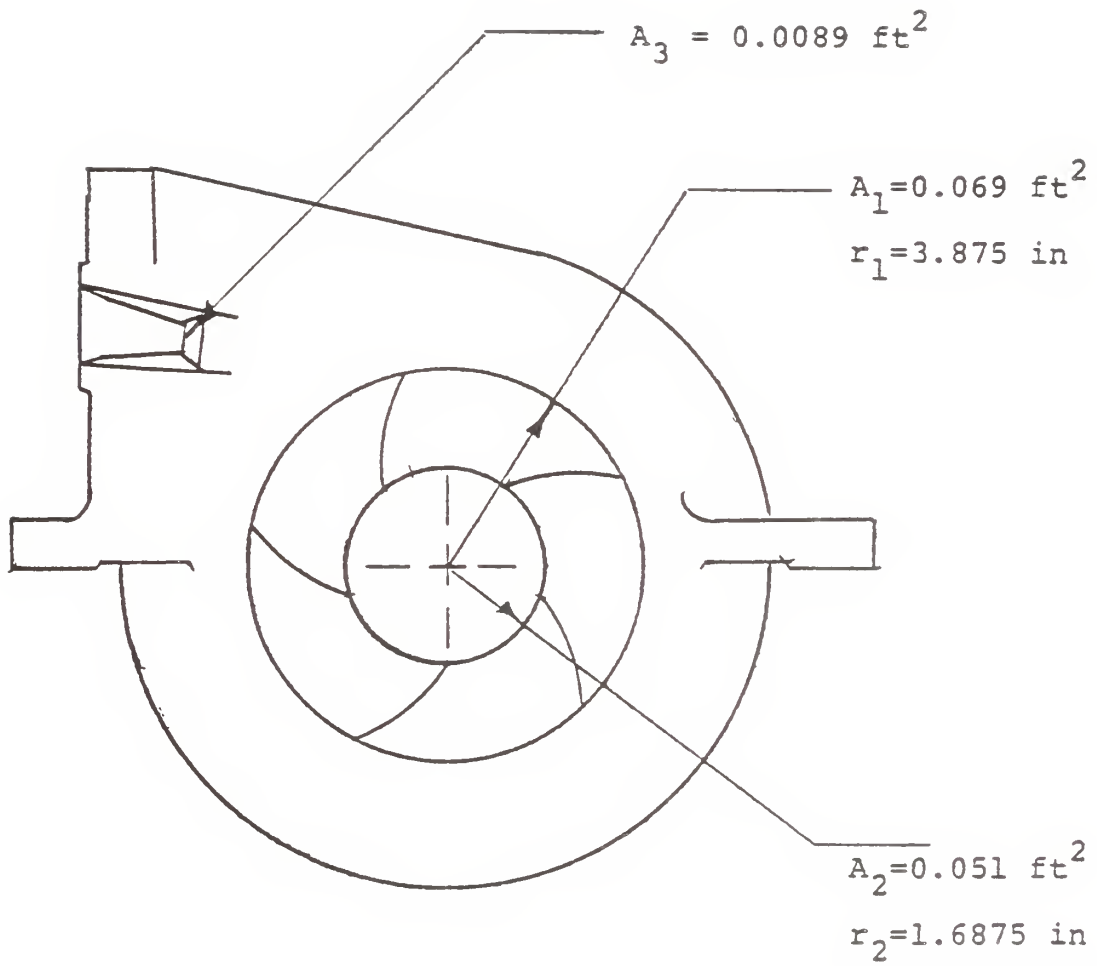

FIGURE 9 - DETAILS OF THE SEMI-SCALE PUMP

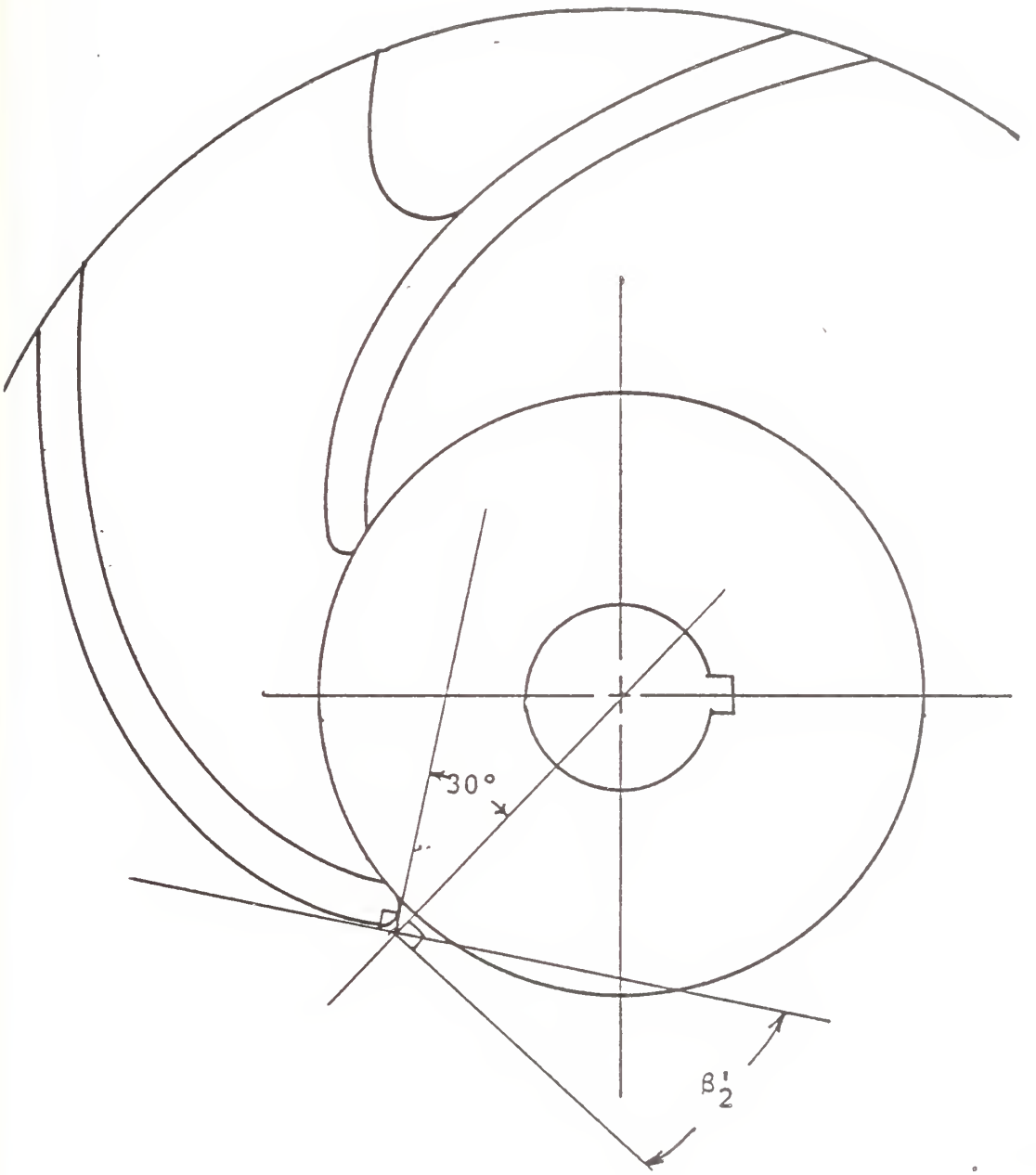

FIGURE 10 - DETAILS OF THE SEMI-SCALE PUMP IMPELLER EYE

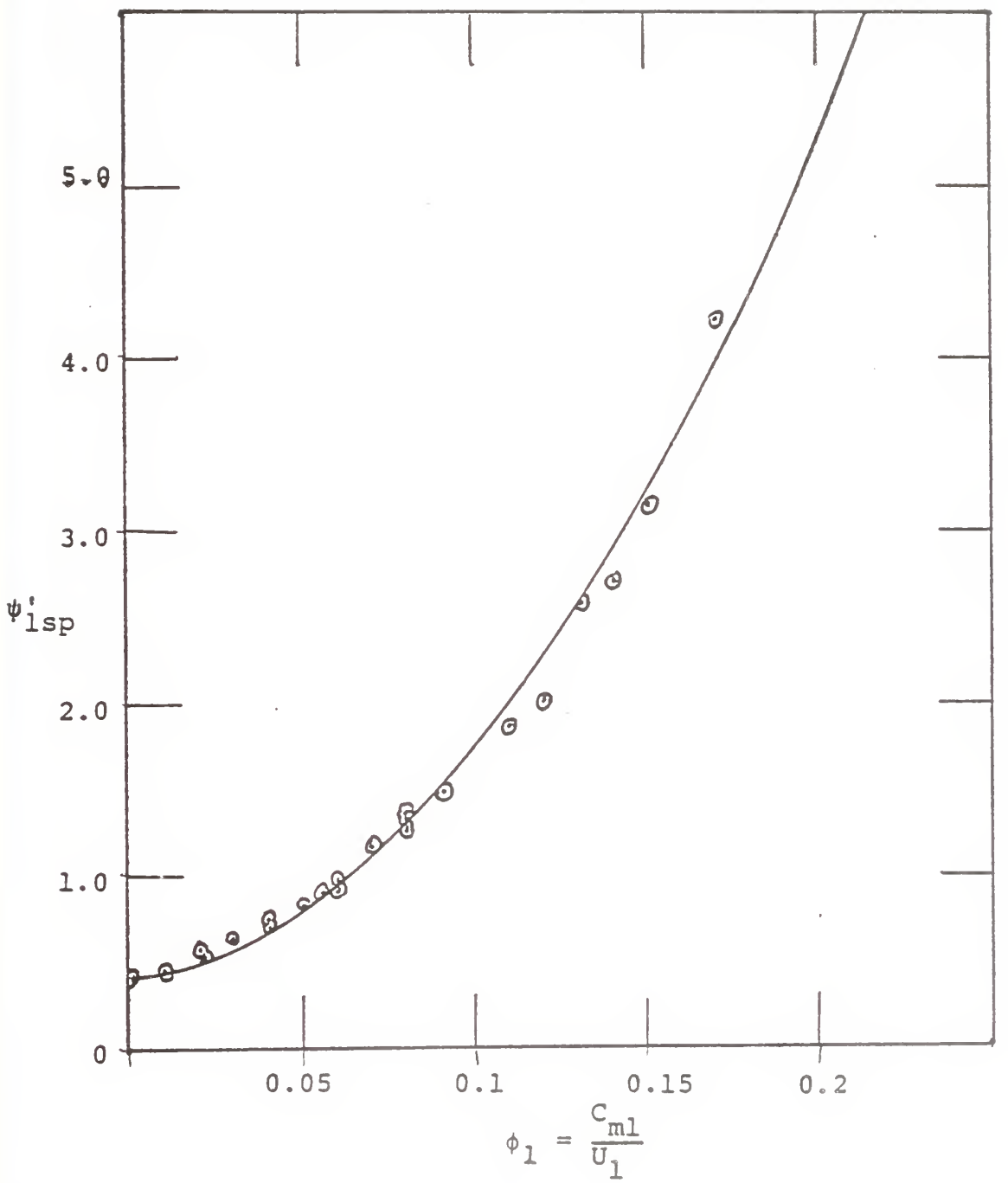

FIGURE 11 - HEAD-VERSUS-FLOW CHARACTERISTICS OF SEMI-SCALE PUMP IN SINGLE-PHASE, THIRD-QUADRANT OPERATION

Head-loss ratio

The head-loss ratio is calculated for each test conducted in two-phase flow, third-quadrant operation.

RESULTS

The results of these calculations are shown in Table 1, and the relationship between head-loss ratio and void fraction for the semi-scale pump is shown in Figure 12.

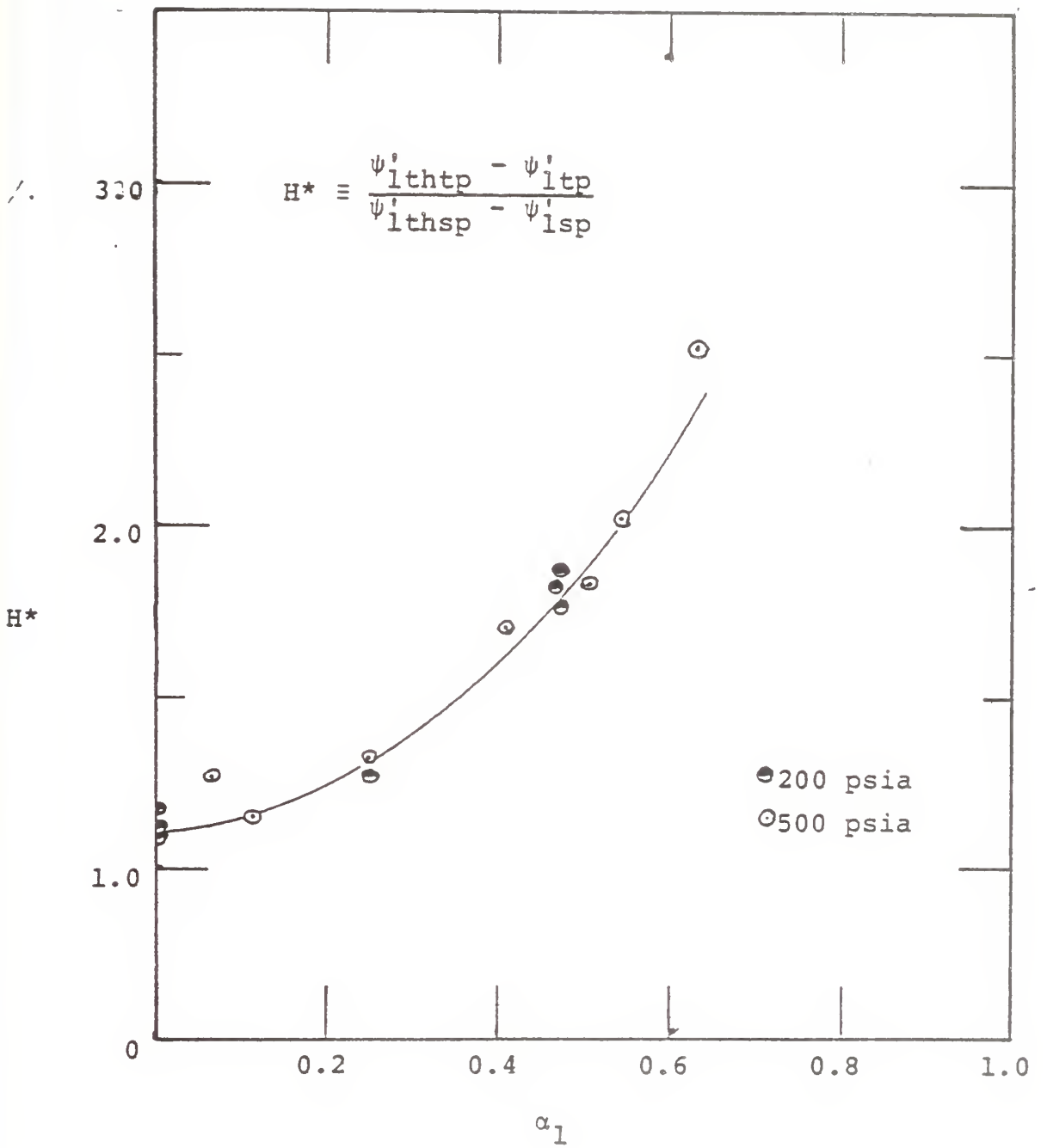

FIGURE 12 - HEAD-LOSS RATIO, H*, VERSUS INLET VOID FRACTION, α_1

TABLE 1

CALCULATION OF HEAD-LOSS RATIO, H*

INLET VOID FRACTION α_1	f_{tpl}	ϕ_{tpl}	ψ'_{lthtp}	ψ'_{ltp}	ψ'_{lthsp}	ψ'_{lsp}	H*
0.461	1.022	0.030	0.095	0.919	0.089	0.545	1.81
0.464	1.015	0.018	-0.022	0.876	-0.025	0.454	1.88
0.466	1.022	0.010	-0.094	0.816	-0.096	0.419	1.77
0	1.0	0.009	-0.102	0.469	-0.102	0.417	1.10
0	1.0	0.010	-0.101	0.481	-0.101	0.417	1.12
0	1.0	0.024	0.027	0.570	0.027	0.491	1.17
0.241	1.015	0.044	0.215	0.824	0.209	0.683	1.28
0.116	1.009	0.047	0.247	0.811	0.244	0.732	1.16
0.245	1.007	0.044	0.214	0.848	0.211	0.686	1.33
0.056	1.004	0.025	0.043	0.629	0.042	0.502	1.27
0.512	1.067	0.037	0.168	1.004	0.146	0.605	1.82
0.537	1.023	0.022	0.012	0.956	0.008	0.476	2.02
0.631	1.033	0.015	-0.048	1.184	-0.052	0.438	2.51
0.401	1.014	0.016	-0.043	0.788	-0.046	0.442	1.70

DISCUSSION

Figure 12 shows that within the range of variables of Olson's experiments, the head-loss ratio of the semi-scale pump in third-quadrant operation correlates very well as a function of inlet void fraction. An average curve drawn through the points can be used to predict the two-phase performance at other values of void fraction, flow, and pressure, up to the maximum void fraction tested.

At low values of void fraction (up to 20%) the flow is largely homogeneous and the losses in two-phase flow are approximately equal to those in single-phase. As void fraction increases above 20%, the flow becomes separated and the relative losses increase sharply, until at the maximum void fraction tested (63%), they are more than twice the single-phase losses. By the definition of the head-loss ratio, its value is unity at a void fraction of 100%; the characteristics between 63%and 100% void-fraction are unknown, but it is reasonable to assume that the head-loss ratio will continue to increase then drop sharply to unity at the very high values of void fraction.

The effect of pressure on the correlation of the head-loss ratio is not apparent for this limited amount of data. Two series of two-phase tests were conducted, one at 200 psia system pressure, the other at 500 psia. The functional

relationship for the head-loss ratio, equation 21, indicated that H* was dependent on void fraction, α, and pressure (for a given pump). In this equation, system pressure affects the two-phase flow function, a, through its effect on density and the slip-velocity ratio, s. Both of these effects are overshadowed by changes in void fraction, α.

OTHER RESULTS

The head-loss ratio was calculated using expressions other than equation 10 for the theoretical two-phase head coefficient.

The experimental data for the fluid properties at pump-outlet were used to evaluate equation 9 and determine the head-loss ratio. Results are shown in Table E1 and Figure E1. These results are not significantly different from the results presented in Figure 12, indicating that the effect of the outlet tangential velocity, $C_{\theta 2}$, is minimal, as assumed. Equation 10 can be applied to any pump, without prior knowledge of the relationships between fluid properties at inlet and exit; therefore, it is much more useful as a means of predicting two-phase characteristics.

Results obtained by assuming zero outlet-swirl are shown in Figure E2, and also show good correlation between H* and α, but indicate much higher losses. The procedure is simplified by this assumption, and further experiments may prove it to be viable for certain pump designs, particularly those of low specific speed.

APPLICATION OF THE PROCEDURE

The two-phase, third-quadrant head-versus-flow characteristics of a centrifugal pump can be predicted, for various values of void fraction and pressure, using the procedure outlined below. The following information concerning the pump must be known.

Flow area at the pump discharge flange, A_3.

Flow area of the outer radius of the impeller, A_1.

Flow area at the impeller eye, A_2.

The impeller radius ratio, r_2/r_1.

Blade angle at impeller eye, β_2', as defined by Figure 3.

Sufficient single-phase data to construct a plot of head-coefficient versus flow-coefficient.

The actual single-phase, and the theoretical single- and two-phase head-versus-flow characteristics are determined by constructing a graph as shown in Figure 13. The three head-coefficients, ψ'_{1sp}, ψ'_{1thsp}, and ψ'_{1thtp}, can then be found for particular values of flow-coefficient, ϕ_1, and two-phase flow function, f_{tp1}.

At the desired value of void fraction, α_1, and system pressure, the head-loss ratio, H*, is determined from Figure 12, and the two-phase flow function, f_{tp1}, calculated.

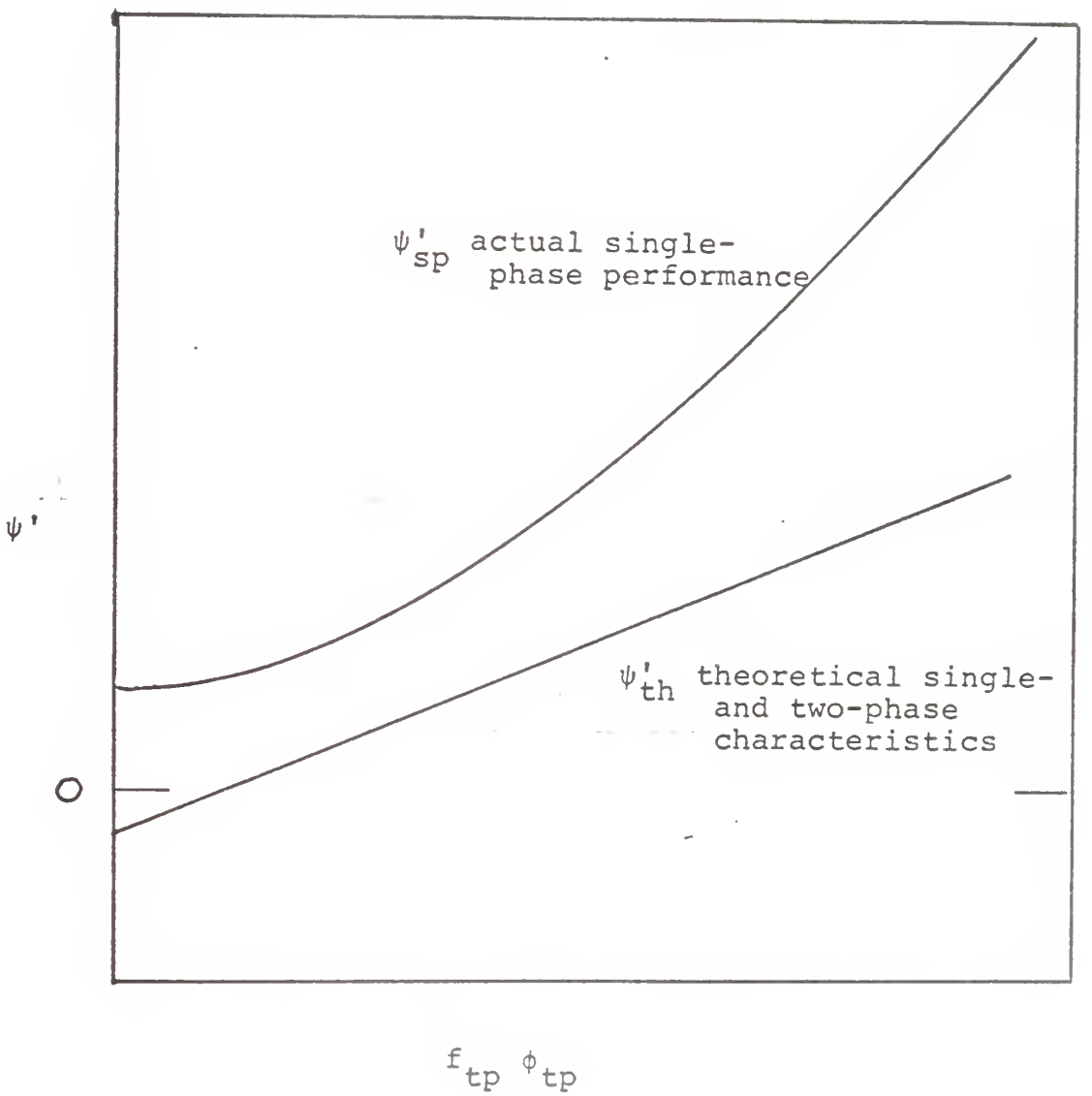

FIGURE 13 - ACTUAL SINGLE-PHASE AND THEORETICAL SINGLE- AND TWO-PHASE PERFORMANCE

The predicted values of actual two-phase head coefficient, ψ'_{ltp}, are calculated as a function of flow-coefficient, ϕ_l, from

$$\psi'_{ltp} = \psi'_{lthtp} - H^*[\psi'_{lthsp} - \psi'_{lsp}]$$

Experiments on pumps of different geometries will be required to determine the effect of geometrical factors such as specific speed, N_s, on the functional relationship of the head-loss ratio, H* (equation 21). Until such data becomes available, this procedure may be used to determine approximate two-phase characteristics.

APPENDIX A

DETAILS OF THE DERIVATION OF THE THEORETICAL TWO-PHASE HEAD COEFFICIENT

In two-phase separated flow, the theoretical two-phase head coefficient is given by

$$\psi'_{1thtp} = \frac{1}{U_1}[(1-x_1)C_{\theta L1}+x_1 C_{\theta v1}]-\frac{U_2}{U_1^2}[(1-x_2)C_{\theta L2}+x_2 C_{\theta v2}] \tag{A1}$$

In general, velocities of the two phases are given by

$$C_L = \frac{\dot{m}_L}{\rho_L A_L} = \frac{\dot{m}_T(1-x)}{\rho_L(1-\alpha)A_T}$$

$$C_v = \frac{\dot{m}_v}{\rho_v A_v} = \frac{\dot{m}_T x}{\rho_v \alpha A_T}$$

Assuming $C_{\theta 1} = C_3$

$$C_{\theta L1} = C_{L3} = \frac{\dot{m}_T(1-x_1)}{\rho_{L1}(1-\alpha_1)A_3}$$

$$C_{\theta v1} = C_{v3} = \frac{\dot{m}_T x_1}{\rho_{v1} \alpha_1 A_3}$$

By continuity

$$\dot{m}_T = \text{constant} = \frac{C_{mL1} \rho_{L1} (1-\alpha_1) A_1}{1 - x_1} = \frac{C_{mv1} \rho_{v1} \alpha_1 A_1}{x_1}$$

Then

$$C_{\theta L1} = \frac{C_{mL1}\ \rho_{L1}(1-\alpha_1)A_1}{(1-x_1)} \quad \frac{(1-x_1)}{\rho_{L1}(1-\alpha_1)A_3}$$

and

$$C_{\theta L1} = C_{mL1}\ \frac{A_1}{A_3}$$

Similarly

$$C_{\theta v1} = C_{mv1}\ \frac{A_1}{A_3}$$

Substituting into equation A1

$$\psi'_{1thtp} = (1-x_1)\frac{C_{mL1}}{U_1} \quad \frac{A_1}{A_3} + x_1\ \frac{C_{mv1}}{U_1}\ \frac{A_1}{A_3} -$$

$$[\frac{(1-x_2)U_2C_{\theta L2}}{U_1^2} + \frac{x_2U_2C_{\theta v2}}{U_1^2}] \qquad \text{(A2)}$$

From the general expressions for velocity

$$C_{mL1} = \frac{\dot{m}_T\ (1-x)}{\rho_{L1}(1-\alpha_1)A_1}$$

and

$$C_{mv1} = \frac{\dot{m}_T\ x_1}{\rho_{v1}\ \alpha_1\ A_1}$$

Substituting these expressions, the first two terms on the right hand side of equation A2 become

$$\frac{(1-x_1)^2\ \dot{m}_T}{U_1 \rho_{L1} (1-\alpha_1) A_1} \frac{A_1}{A_3} + \frac{x_1^2\ \dot{m}_T}{\rho_{v1}\ \alpha_1\ U_1 A_1} \frac{A_1}{A_3}$$

Rearranging and multiplying by

$$\frac{(1-\alpha_1)\ \rho_{L1} + \alpha_1\ \rho_{v1}}{(1-\alpha_1)\ \rho_{L1} + \alpha_1\ \rho_{v1}}$$

where

$$(1-\alpha)\rho_L + \alpha\rho_v \equiv \rho_{tp}$$

They become

$$\frac{\dot{m}_T\ A_1}{U_1\ \rho_{tp1}\ A_1\ A_3} \left[\frac{(1-x_1)^2}{\rho_{L1}(1-\alpha_1)} + \frac{x_1^2}{\rho_{v1}\ \alpha_1}\right]\left[(1-\alpha_1)\ \rho_{L1} + \alpha_1\ \rho_{v1}\right]$$

Substituting the definition of the two-phase flow coefficient

$$\phi^1_{tpv} = \frac{\dot{m}_T}{\rho_{tp1}\ A_1\ U_1}$$

the two terms become

$$\frac{A_1}{A_3}\ \phi_{tp1}\ \left[(1-x_1)^2 + \frac{(1-x_1)^2\ \alpha_1\ \rho_{v1}}{\rho_{L1}(1-\alpha_1)} + \frac{x_1^2\ \rho_{L1}\ (1-\alpha_1)}{\rho_{v1}\ \alpha_1} + x_1^2\right]$$

by definition, the two-phase flow function, a, is

$$a \equiv \left[\frac{\alpha}{1-\alpha}\right] \frac{\rho_v}{\rho_L}$$

and the quality, x, becomes

$$x = \frac{as}{1+as}$$

where

$$s \equiv \frac{C_v}{C_L}$$

substituting these expressions, the first two terms become

$$\frac{A_1}{A_3} \phi_{tp1} [1+a_1][1-\frac{2a_1s_1}{1+a_1s_1} + \frac{(a_1s_1)^2}{1+2a_1s_1+(a_1s_1)^2} (1+ \frac{1}{a})]$$

performing the indicated operations and rearranging yields

$$\frac{A_1}{A_3} \phi_{tp1} \frac{(1+a_1)(1+a_1s_1^2)}{(1+a_1s_1)^2}$$

Substituting this expression, equation A2 becomes

$$\psi'_{1thtp} = \frac{A_1}{A_3} \phi_{tp1} f_{tp1} - [\frac{(1-x_2)U_2C_{\theta L2}}{U_1^2} + \frac{x_2U_2C_{\theta v2}}{U_1^2}]$$

where

$$f_{tp1} \equiv \frac{(1+a_1)(1+a_1 s_1^2)}{(1+a_1 s_1)^2}$$

From the outlet velocity triangle, Figure 4, the last two terms in equation A2 reduce to

$$[1 - \frac{f_{tp2}\ \phi_{tp2}}{\tan \beta_2}] (\frac{r_2}{r_1})^2$$

using the same procedure applied to the first two terms. Equation A2 becomes

$$\psi'_{1thtp} = \frac{A_1}{A_3} \phi_{tp1}\ f_{tp1} - (\frac{r_2}{r_1})^2\ [1 - \frac{f_{tp2}\ \phi_{tp2}}{\tan \beta_2}]$$

The two-phase flow coefficients, ϕ_{tp}, at inlet and outlet can be related by the continuity equation,

$$\phi_{tp2} = \phi_{tp1} \frac{\rho_{tp1}}{\rho_{tp2}}\ \frac{A_1}{A_2}\ \frac{U_1}{U_2}$$

Substituting this expression and rearranging yields

$$\psi'_{1thtp} = -(\frac{r_2}{r_1})^2 + [\frac{A_1}{A_3} f_{tp1} + \frac{r_2}{r_1} \frac{\rho_{tp1}}{\rho_{tp2}} \frac{A_1}{A_2} \frac{f_{tp2}}{\tan \beta_2}]\ \phi_{tp1} \qquad \text{(A3)}$$

APPENDIX B

DETAILS OF THE CALCULATION OF HEAD-LOSS RATIO, H*

The head-loss ratio, H*, for the various values of void fraction, α, was calculated using the relationships previously presented. The data from the experiments conducted by Olson are included in Appendix C. Values for fluid densities were interpolated from reference 9.

Table B1 lists the single-phase characteristics used to determine the single-phase head coefficient, ψ'_{lsp}, as a function of flow coefficient, ϕ_l. Tables B2 through B5 present the calculation of the head-loss ratio, H*.

The test number column refers to the experimental data.

TABLE B1

CALCULATION OF THE SINGLE-PHASE HEAD COEFFICIENT, ψ'_{1sp}, AS A FUNCTION OF FLOW COEFFICIENT, ϕ_1

SINGLE-PHASE TEST NUMBER	$g\Delta H$ (ft^2/sec^2)	U_1 (ft/sec)	C_{m1} (ft/sec)	ψ'_{1sp} ($g\Delta H/U_1^2$)	ϕ_1 (C_{m1}/U_1)
78	1330	13.2	3.188	7.64	0.24
82	1459	14.2	3.275	7.22	0.23
86	164.22	13.4	0.75	0.91	0.06
87	570	13.5	1.962	3.15	0.15
88	763	13.5	2.308	4.22	0.17
89	1346	13.6	3.188	7.40	0.23
92	74	13.6	0	0.4	0
83	4176	20.8	3.635	9.63	0.17
75	605	27.1	1.255	0.82	0.05
76	960	27.2	2.121	1.30	0.08
77	1513	27.1	3.231	2.06	0.12
91	299.5	27.04	0	0.41	0
95	2380	53.78	2.568	0.82	0.05
98	1204	54.15	0	0.41	0
150	4405	54.25	4.95	1.50	0.09
106	3130	74.6	1.414	0.56	0.02
107	3916	74.7	2.640	0.70	0.04
108	4634	74.6	3.534	0.83	0.05
149	7065	74.5	5.756	1.27	0.08
147	7467	90.9	5.02	0.90	0.055
148	9792	91.2	6.492	1.18	0.07
152	9982	92.0	6.65	1.18	0.07

TABLE B2

CALCULATION OF TWO-PHASE FLOW FUNCTION, f_{tp}, AND TWO-PHASE DENSITY, ρ_{tp}, AT PUMP INLET

TWO-PHASE TEST NUMBER	VAPOR DENSITY ρ_{vl} lb_m/ft^3	LIQUID DENSITY ρ_{Ll} lb_m/ft^3	VOID FRACTION α_l	f_{tpl}	ρ_{tpl} lb_m/ft^3
149	0.4377	54.38	0.548	1.0299	24.82
150	0.4443	54.33	0.461	1.0218	29.49
151	0.4508	54.28	0.464	1.0151	29.30
152	0.4354	54.40	0.466	1.0218	29.25
153	0.4354	54.40	0**	1.0	54.40
154	0.4420	54.35	0**	1.0	54.35
155	0.4309	54.43	0**	1.0	54.43
156	0.4288	54.45	0.241	1.0150	41.43
*					
157	1.1002	50.53	0.116	1.0086	44.80
158	1.1066	50.51	0.245	1.0069	38.41
159	1.1042	50.52	0.056	1.0039	47.75
160	1.0932	50.57	0.512	1.0671	25.24
161	1.1156	50.46	0.537	1.0232	23.96
162	1.1156	50.46	0.631	1.0327	19.32
163	1.1453	50.33	0.401	1.0143	30.61
164	1.1202	50.44	0.647	1.0348	18.53

*Tests 149 through 156 were conducted at nominal system pressure of 200 psia, from Figure 5, slip velocity ratio, s = 2.8. Tests 157 through 164 were conducted at nominal system pressure of 500 psia, s = 2.

**Negative void fractions in data were taken to be zero.

TABLE B3

CALCULATION OF TWO-PHASE FLOW FUNCTION, f_{tp}, AND TWO-PHASE DENSITY, ρ_{tp}, AT PUMP OUTLET

TWO-PHASE TEST NUMBER	VAPOR DENSITY ρ_{v2} lb_m/ft^3	LIQUID DENSITY ρ_{L2} lb_m/ft^3	VOID FRACTION α_2	f_{tp2}	ρ_{tp2} lb_m/ft^3
149	0.4261	54.47	0.840	1.1070	9.07
150	0.4113	54.60	0.867	1.1234	7.62
151	0.4197	54.52	0.781	1.0767	12.27
152	0.4197	54.52	0.558	1.0298	24.33
153	0.4009	54.68	0.008	1.0002	54.25
154	0.3967	54.71	0.007	1.0002	54.33
155	0.3946	54.73	0.730	1.0568	15.07
156	0.3864	54.80	0.789	1.0742	11.87
157	1.0514	50.76	0.702	1.0405	15.86
158	1.0646	50.70	0.756	1.0509	13.18
159	1.0624	50.71	0.428	1.0147	29.46
160	1.0646	50.70	0.696	1.0400	16.15
161	1.0844	50.61	0.912	1.1065	5.44
162	1.0844	50.61	0.988	1.0860	1.68
163	1.1173	50.46	0.744	1.0505	13.75
164	1.0998	50.54	0.834	1.0736	9.31

$$f_{tp} = \frac{(1+a)(1+as^2)}{(1+as)^2}$$

$$a = \left(\frac{\alpha}{1-\alpha}\right) \frac{\rho_v}{\rho_L}$$

$$\rho_{tp} = (1-\alpha)\ \rho_L + \alpha\rho_v$$

TABLE B4

CALCULATION OF TWO-PHASE FLOW COEFFICIENT, ϕ_{tpl}, AND TWO-PHASE HEAD COEFFICIENT, ψ'_{ltp}

TWO-PHASE TEST NUMBER	FLOW RATE, Q (gal/min)	ROTOR SPEED, N (rev/min)	ϕ_{tpl} (0.951 Q/N)	HEAD ΔH_o (ft)	ψ'_{ltp} $(28{,}200 \frac{\Delta H_o}{N^2})$
149	-85.9	0	--	40.2	--
150	-51.5	-1608	0.030	84.3	0.919
151	-30.3	-1600	0.018	79.6	0.876
152	-17.3	-1607	0.010	74.8	0.816
153	-16.2	-1604	0.009	42.8	0.469
154	-16.4	-1602	0.010	43.8	0.481
155	-39.8	-1600	0.024	51.8	0.570
156	-73.4	-1603	0.044	75.1	0.824
157	-80.0	-1607	0.047	74.3	0.811
158	-73.8	-1603	0.044	77.3	0.848
159	-42.6	-1600	0.025	57.1	0.629
160	-61.4	-1594	0.037	90.5	1.004
161	-36.2	-1597	0.022	86.5	0.956
162	-25.3	-1600	0.015	107.5	1.184
163	-26.5	-1603	0.016	71.8	0.788
164	-112.9	0	--	76.4	--

TABLE B5

CALCULATION OF HEAD-LOSS RATIO, H*

TWO-PHASE TEST NUMBER	ψ'_{lthtp}	ψ'_{ltp}	ψ'_{lthsp}	ψ'_{lsp}	H*	INLET VOID FRACTION α_l
149	--	--	--	--	--	--
150	0.095	0.919	0.089	0.545	1.81	0.461
151	-0.022	0.876	-0.025	0.454	1.88	0.464
152	-0.094	0.816	-0.096	0.419	1.77	0.466
153	-0.102	0.469	-0.102	0.417	1.10	0
154	-0.101	0.481	-0.101	0.417	1.12	0
155	0.027	0.570	0.027	0.491	1.17	0
156	0.215	0.824	0.209	0.683	1.28	0.241
157	0.247	0.811	0.244	0.732	1.16	0.116
158	0.214	0.848	0.211	0.686	1.33	0.245
159	0.043	0.629	0.042	0.502	1.27	0.056
160	0.168	1.004	0.146	0.605	1.82	0.512
161	0.012	0.956	0.008	0.476	2.02	0.537
162	-0.048	1.184	-0.052	0.438	2.51	0.631
163	-0.043	0.788	-0.046	0.442	1.70	0.401
164	--	--	--	--	--	--

$$\psi'_{lth} = -0.1896 + 9.155\, f_{tpl}\, \phi_l$$

$$\psi'_{lsp} = 101.28\, \phi_l^{1.8756} + 0.4$$

$$H^* = \frac{\psi'_{lthtp} - \psi'_{ltp}}{\psi'_{lthsp} - \psi'_{lsp}}$$

APPENDIX C

EXPERIMENTAL DATA

Tables C1 and C2 are reproduced from reference 7.

Explanatory notes for single-phase tests:

a. Based on turbine flowmeter measurements.

b. Positive pump ΔP represents higher pressure at discharge nozzle.

c. Based on fluid density measurement at pump inlet.

d. Fluid density at pump inlet (suction for normal operation, discharge for reverse flow).

e. Inlet and outlet refer to locations with respect to direction of flow.

f. Flow rate obtained from venturi flowmeter in test loop.

Explanatory notes for two-phase tests:

a. Inlet flow based on loop mass flow rate and test section inlet (suction or discharge) fluid density.

b. Positive ΔP indicates higher pressure at pump discharge.

c. Based on inlet conditions.

d. Inlet and outlet refer to the direction of flow.

e. Calculated using measured density and assumed saturation conditions.

f. Measured directly.

TABLE C1 (from reference 7)

RESULTS OBTAINED FROM TEST SECTION MEASUREMENTS DURING SINGLE-PHASE PLOW PUMP TESTS

Test	Impeller Speed (rpm)	Volumetric Flow Rate[a] (gpm)	Pump Head (psid)[b]	Pump Head (ft of fluid)[c]	Density[d] (lb/ft^3)	Torque (in./lb)	Fluid Temperature (°F) Pump Inlet[e]	Fluid Temperature (°F) Pump Outlet[e]	Pressure (psig) Pump Inlet[e]	Pressure (psig) Pump Outlet[e]
066	1599	-88	26.7	61.9	62.0	100.0	99.4	99.0	93.1	69.5
067	1602	0	20.0	46.5	62.0	87.9	97.2	99.4	58.4	75.9
068	798	0	5.0	11.6	62.0	46.5	94.1	97.2	56.4	58.7
069	798	-38	6.1	14.2	62.1	50.2	96.3	95.9	67.8	62.4
070	799	-48	7.3	17.0	62.0	52.6	97.6	97.2	73.9	66.5
071	801	-69	11.0	25.6	62.0	62.4	99.8	99.4	73.9	66.5
072	801	-101	21.3	49.5	62.0	90.3	99.8	99.4	92.1	73.5
073	800	-139	35.1	90.7	62.1	135.4	96.8	96.3	120.4	83.6
074	2204	-110	47.6	110.3	62.1	142.8	94.1	94.1	124.5	81.6
075	-802	-39	8.1	18.8	62.1	-39.1	95.4	94.6	68.8	63.4
076	-804	-66	12.8	29.8	62.0	-27.5	99.4	99.0	81.0	70.5
077	-802	-100.4	20.2	47.0	62.0	0.1	98.5	98.1	98.2	79.6
078	-390	-99	17.8	41.3	62.2	18.6	85.3	84.9	82.0	67.5
079	-206	-86	12.7	29.5	62.2	15.9	86.6	86.2	82.0	71.5
080	0	-64	7.2	16.7	62.2	11.6	89.7	89.3	68.8	64.4
081	-246	-92	14.5	33.7	62.1	16.8	92.3	91.9	86.0	74.5
082	-420	-102	19.5	45.3	62.1	18.6	94.6	94.1	96.1	79.6
083	-616	-113	55.9	129.7	62.1	22.3	96.3	95.9	100.2	78.5
084	-865	-121	29.7	68.8	62.1	20.5	97.6	97.6	110.3	84.6
085	-1194	-137	41.1	95.3	62.1	23.3	97.6	97.6	132.6	95.7
086	-397	-23.3[f]	2.2	5.1	62.1	-21.4	96.3	95.9	60.7	61.4
087	-398	-61	7.6	17.7	62.1	-7.0	96.8	96.3	65.8	62.4

TABLE C1 (cont)

RESULTS OBTAINED FROM TEST SECTION MEASUREMENTS DURING SINGLE-PHASE PLOW PUMP TESTS

Test	Impeller Speed (rpm)	Volumetric Flow Rate[a] (gpm)	Pump Head (psid)[b]	Pump Head (ft of fluid)[c]	Density[d] (lb/ft^3)	Torque (in./lb)	Fluid Temperature (°F) Pump Inlet[e]	Fluid Temperature (°F) Pump Outlet[e]	Pressure (psig) Pump Inlet[e]	Pressure (psig) Pump Outlet[e]
088	-398	-72	10.2	23.7	62.1	0	96.8	96.3	70.8	64.4
089	-399	-99	18.0	41.8	62.1	16.8	98.5	98.1	88.0	72.5
090	-800	-118	26.3	61.2	62.0	18.6	99.8	99.4	103.2	78.5
091	-800	0	4.0	9.3	62.0	-45.6	99.8	97.6	60.7	60.4
092	-403	0	1.0	2.3	62.0	-25.6	99.0	99.4	58.7	60.4
093	-1602	-31	21.2	49.2	62.2	-72.1	80.9	80.9	88.0	66.5
094	-1594	-47	24.4	56.7	62.1	-69.8	96.8	96.3	98.2	73.5
095	-1591	-80	31.9	73.9	62.1	-50.2	95.9	95.4	114.4	82.6
096	-1595	-101	38.3	88.8	62.1	-34.0	92.3	91.9	126.5	87.6
097	-1602	-134	53.0	122.7	62.2	-3.3	84.4	84.4	157.9	107.7
098	-1602	0	16.1	37.4	62.2	-92.1	84.9	84.4	72.9	58.4
099	-2197	0	29.9	69.1	62.2	-131.7	83.5	84.4	86.0	56.4
100	-2704	-29[f]	52.1	120.7	62.2	-140.0	91.0	91.0	126.5	76.5
101	-2699	-47	58.9	136.6	62.1	-131.2	93.7	93.7	133.6	74.5
102	-2697	-78.4	70.3	163.2	62.1	-11.7	95.4	95.4	155.8	88.6
103	-2699	-109	81.0	187.8	62.1	-87.0	95.4	95.9	173.1	93.7
104	-2698	-133	92.9	215.1	62.2	-59.1	86.2	86.2	198.4	104.7
105	-2706	0	44.9	104.1	62.1	-168.0	97.6	103.4	99.2	50.4
106	-2208	-44	41.9	97.2	62.1	-90.7	98.5	98.5	112.3	68.5
107	-2210	-82	52.4	121.6	62.1	-67.9	93.7	93.7	135.6	80.6
108	-2208	-110	62.1	143.9	62.2	-46.1	90.1	90.1	152.8	88.6
109	-2206	-137	73.7	170.1	62.2	-20.0	87.5	87.5	174.1	99.7

TABLE C1 (cont)

RESULTS OBTAINED FROM TEST SECTION MEASUREMENTS DURING SINGLE-PHASE FLOW PUMP TESTS

Test	Impeller Speed (rpm)	Volumetric Flow Rate[a] (gpm)	Pump Head		Density[d] (lb/ft^3)	Torque (in./lb)	Fluid Temperature (°F)		Pressure (psig)	
			(psid)[b]	(ft of fluid)[c]			Pump Inlet[e]	Pump Outlet[e]	Pump Inlet[e]	Pump Outlet[e]
132	-2190	142	-5.1	-11.9	62.0	-313.6	97.6	98.1	71.5	64.8
133	-1604	81	3.3	7.7	62.1	-155.9	96.3	96.8	56.3	59.7
134	-1601	103	-2.6	-6.0	62.1	-188.0	96.8	96.8	65.5	62.7
135	-1599	137	-13.2	-30.7	62.1	-227.5	96.3	96.8	78.5	64.8
136	0	149	-18.8	-43.7	62.1	2.8	95.9	95.9	86.6	67.8
137	-796	196	-37.8	-87.5	62.2	-165.8	90.6	91.0	115.8	74.9
138	-794	195	-38.5	-88.9	62.4	-168.0	91.5	91.9	111.8	67.8
139	-1599	171	-25.3	-58.3	62.4	-279.2	95.0	95.9	92.6	63.8
140	-1595	207	-39.5	-91.2	62.4	-316.4	99.4	99.0	113.8	69.8
141	-1588	258	-66.7	-154.2	62.3	-384.3	98.1	98.5	153.1	81.0
142	-2704	159	0	0	62.2	-430.9	92.8	99.4	65.5	61.7
143	-2205	141	-6.2	-14.4	62.0	-327.6	91.9	92.8	72.5	62.7
144	-2197	186	-23.0	-53.2	62.3	-386.2	92.3	92.8	97.7	69.8
145	-2198	226	-42.7	-99.8	61.6	-446.2	92.8	93.7	126.9	79.9
146	191	238	-46.7	-107.9	62.3	-14.9	92.3	92.8	130.9	78.9
147	-2690	-156	100.4	231.9	62.3	-39.6	77.8	77.8	181.1	82.6
148	-2698	-202	131.7	304.1	62.4	26.5	80.9	80.5	210.5	81.6
149	-2204	-179	95.0	219.4	62.4	23.3	83.1	82.7	168.0	75.5
150	-1605	-154	59.1	136.8	62.2	23.3	84.4	83.5	125.5	66.5
151	-2197	-187	97.7	225.7	62.3	26.1	85.3	84.9	173.1	75.7
152	-2722	-207	134.0	310.0	62.2	31.6	86.6	86.2	216.6	84.6
153	801	-195	75.3	173.8	62.3	220.1	85.3	85.3	147.8	75.5

TABLE C2 (from reference 7)

RESULTS OBTAINED FROM TEST SECTION MEASUREMENTS DURING TWO-PHASE FLOW PUMP TESTS

Test	Nominal System Pressure (psia)	Pump Impeller Speed (rpm)	Flow Rate		Head		Density (lb/ft^3)		Void Fraction[e]		Torque[f]	Temperature (°F)		Pressure (psig)	
			Test Section (gpm)[a]	Loop (lb/hr)	(psid)[b]	(ft of fluid)[c]	Pump inlet[d]	Pump outlet[d]	Pump inlet[d]	Pump outlet[d]	(in./lb)	Pump inlet[d]	Pump outlet[d]	Pump inlet[d]	Pump outlet[d]
146	200	2712	-43.2	-9836	51.8	262.3	28.4	3.27	0.483	0.946	129.35	379.5	354.5	190.9	141.1
147	200	2700	-29.0	-6382	53.1	279.1	27.4	3.12	0.502	0.949	128.89	376.9	353.1	185.7	135.1
148	200	2703	-56.6	-23874	57.1	156.1	52.63	5.12	0.036	0.902	127.03	377.4	351.4	186.7	133.1
149	200	0	-85.9	-17162	7.0	40.2	24.9	9.11	0.548	0.840	1.86	378.1	375.2	185.7	180.2
150	200	-1608	-51.5	-12235	17.3	84.3	29.6	7.62	0.461	0.867	-68.86	378.0	371.6	188.8	173.2
151	200	-1600	-30.3	-7132	16.3	79.6	29.4	12.3	0.464	0.781	-73.05	381.3	373.8	191.9	177.2
152	200	-1607	-17.3	-4066	15.2	74.8	29.3	24.2	0.466	0.558	-74.91	377.8	371.6	184.6	172.2
153	200	-1604	-16.2	-7168	16.4	42.8	55.3	54.4	-0.013	0.008	-72.12	375.6	370.3	184.6	168.2
154	200	-1602	-16.4	-6875	16.9	43.8	55.5	54.5	-0.014	0.007	-72.12	373.0	369.0	187.7	166.2
155	200	-1600	-39.8	-17615	19.9	51.8	52.2	15.1	-0.011	0.730	-64.68	376.0	369.9	182.5	165.2
156	200	-1603	-73.4	-24429	21.6	75.1	41.5	11.9	0.241	0.789	-56.30	379.1	369.0	181.5	161.2
157	500	-1607	-80.0	-28884	23.2	74.3	45.0	15.9	0.116	0.702	-58.63	464.1	458.4	495.7	473.5
158	500	-1603	-73.8	-22842	20.7	77.3	38.6	13.2	0.245	0.756	-65.61	464.1	459.3	498.6	479.5
159	500	-1600	-42.6	-16444	19.1	57.1	48.1	29.6	0.056	0.428	-73.05	462.4	458.8	497.5	478.5
160	500	-1594	-61.4	-12449	15.9	90.5	25.3	16.2	0.512	0.696	-69.80	464.1	459.7	492.5	479.5
161	500	-1597	-36.2	-7001	14.5	86.5	24.1	5.38	0.537	0.912	-79.10	464.1	460.1	502.7	488.5
162	500	-1600	-25.3	-3942	14.5	107.5	19.4	1.57	0.631	0.988	-87.48	464.1	460.1	502.7	488.5
163	500	-1603	-26.5	-6569	15.4	71.8	30.9	13.5	0.401	0.744	-79.10	461.1	452.9	516.3	503.5
164	500	0	-112.9	-16846	10.0	76.4	18.85	9.33	0.647	0.834	0	464.6	461.9	504.8	495.5
165	500	2684	-138.0	-19590	36.3	294.6	17.7	7.85	0.666	0.868	118.19	462.8	454.9	495.4	461.5
166	500	2701	-66.1	-12088	45.1	284.1	22.8	6.94	0.563	0.882	115.86	463.7	453.6	501.7	459.5
167	500	2706	-46.8	-9676	46.3	258.4	25.8	6.87	0.502	0.882	117.26	464.6	454.0	509.0	466.5
168	500	2703	-29.2	-6182	47.6	259.1	26.4	7.34	0.490	0.874	117.72	464.1	453.1	501.7	460.6
169	500	2694	-66.2	-22819	53.1	177.7	43.0	22.8	0.156	0.566	120.05	464.1	452.2	504.8	454.5
170	200	2687	101.3	5201	-0.15	-3.27	6.42	9.47	0.889	0.833	66.07	378.2	379.1	194.2	188.8
171	200	1593	78.2	4702	-0.58	-11.2	7.51	9.47	0.869	0.833	50.72	378.7	378.7	197.2	190.9
172	200	2717	88.3	4816	-0.29	-6.22	6.76	9.63	0.882	0.830	65.14	379.1	379.1	196.2	190.9
173	200	2712	83.0	3796	0.15	3.68	5.73	9.63	0.902	0.830	62.35	376.9	377.4	192.2	189.9
174	200	2707	79.0	3993	0.15	3.35	6.29	9.45	0.891	0.824	63.75	377.8	378.2	185.2	185.7
175	200	1596	78.0	3942	-0.56	-12.75	6.28	10.26	0.892	0.818	50.72	377.8	378.7	194.2	187.7

APPENDIX D

DESCRIPTION OF EXPERIMENTS

The semi-scale pump used in the experiments had the following characteristics:

Rated flow - 180 gpm

Rated head - 192 ft.

Specific speed - 926

Rated torque - 417.6 in-lb

Details of the pump are shown in Figures 9 and 10.

The test-loop used for single-phase tests is shown in Figure D1. The two-phase test-loop is shown in Figure D2. Superheated steam and/or saturated water were supplied by an oil-fired boiler.

Flow conditions imposed for third quadrant tests are as follows.

Single-phase tests

Impeller speed - up to minus 2700 rpm

Flow rate - 0 to minus 207 gpm

Pressure at pump inlet - 60.7 to 216.6 psig

Pump head - 5.1 to 310.0 ft of fluid

Two-phase tests

Impeller speed - 0 and minus 1600 rpm

Flow rate - minus 16.2 to minus 112.9 gpm

System pressure - 200 and 500 psia

Pump head - 40.2 to 107.5 ft of fluid

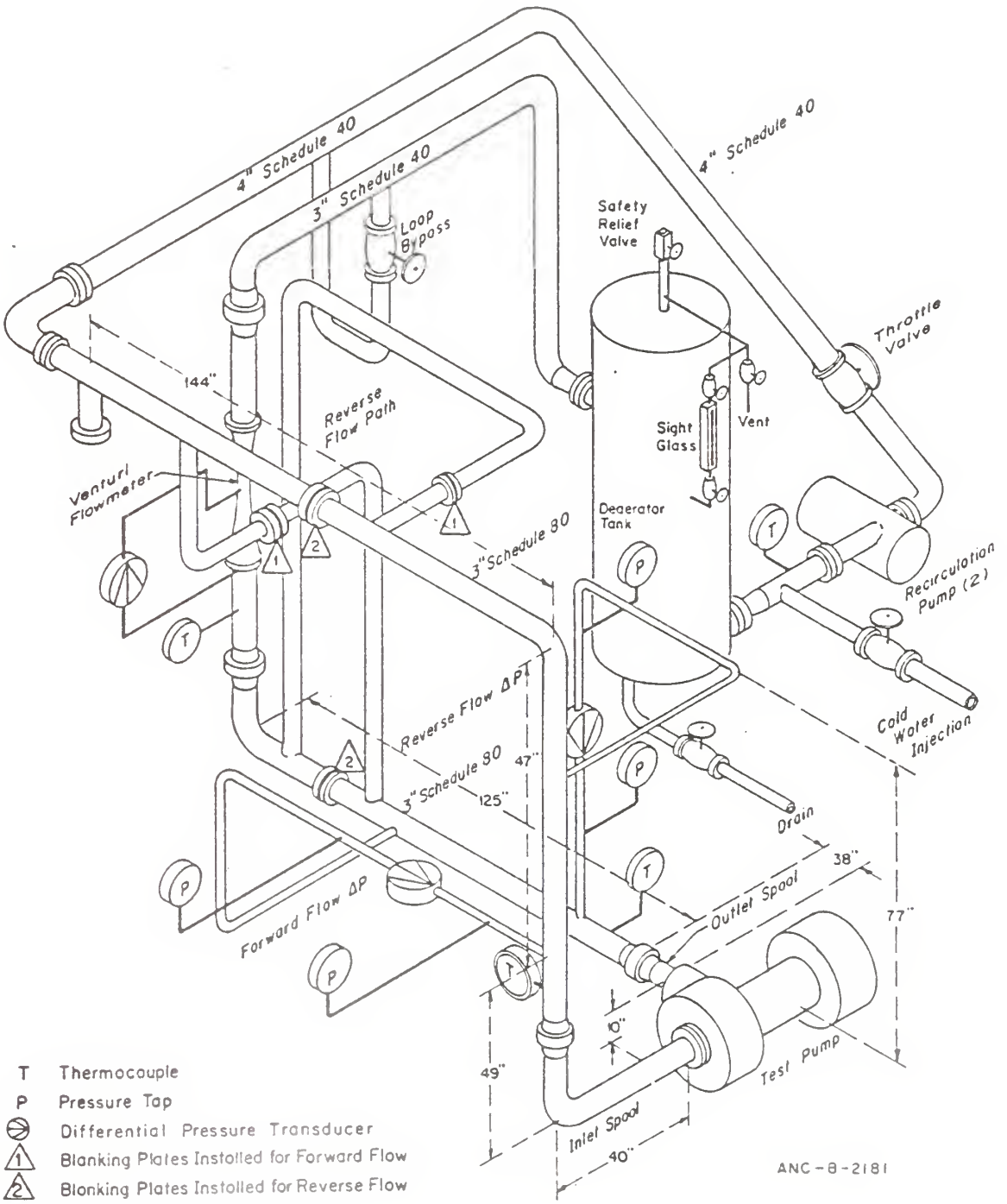

FIGURE D1 - SINGLE-PHASE TEST LOOP (from reference 7)

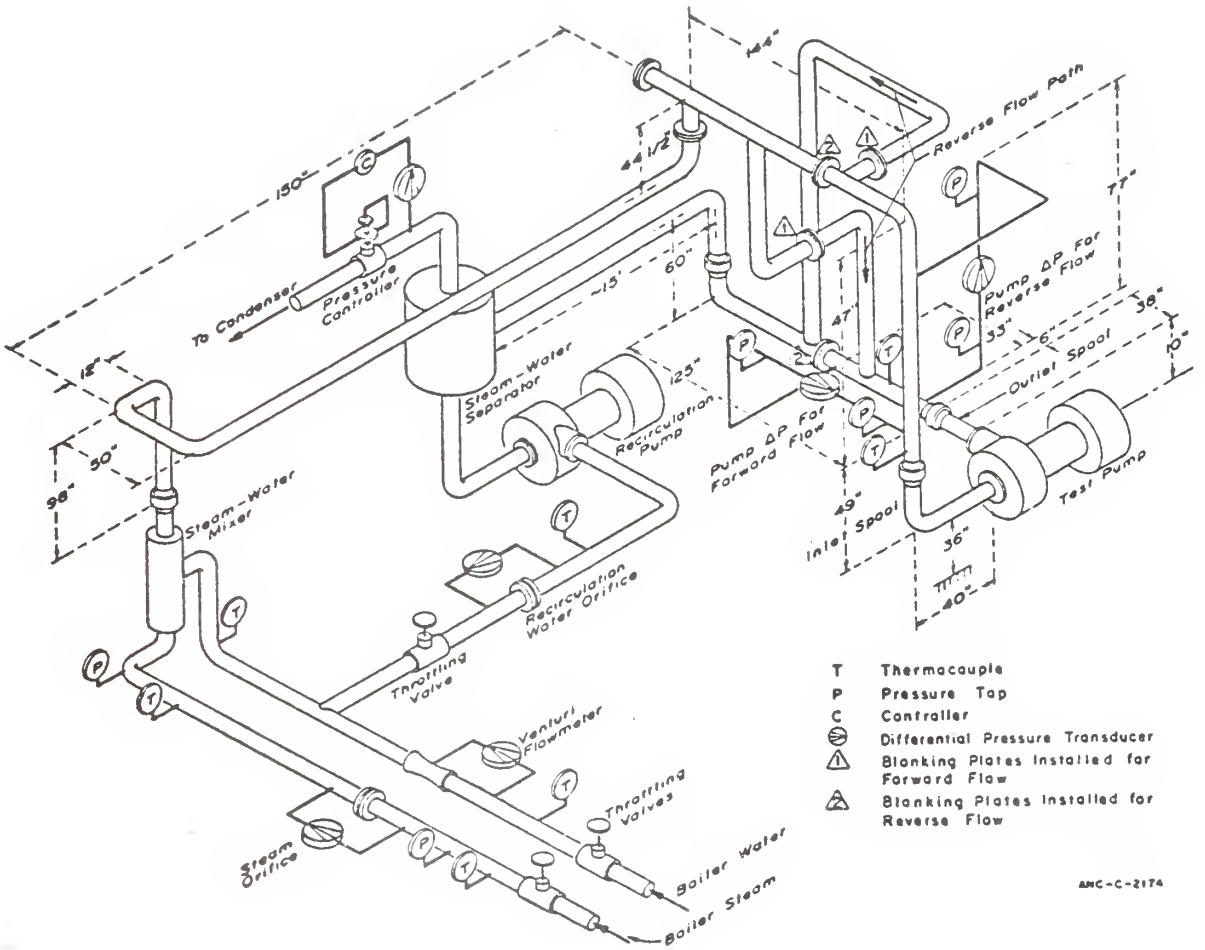

FIGURE D2 - TWO-PHASE TEST LOOP (from reference 7)

APPENDIX E

OTHER RESULTS

This section summarizes, for purposes of comparison, the correlation of H* vs α obtained using alternate methods to compute the theoretical characteristics.

The experimental data were used to evaluate equation 9, thereby making it semi-empirical rather than theoretical. The head coefficients obtained in this manner were used to calculate the head-loss ratio. Results are shown in Table E1 and Figure E1.

ZERO SWIRL AT OUTLET

The theoretical characteristics can be derived assuming that outlet swirl is negligible. In this case the expression for the theoretical head coefficient, ψ'_{1th}, is

$$\psi'_{1th} = \frac{A_1}{A_3} \; f_{tp1} \; \phi_1$$

Results are shown in Table E2, and the correlation of H* versus α is shown in Figure E2.

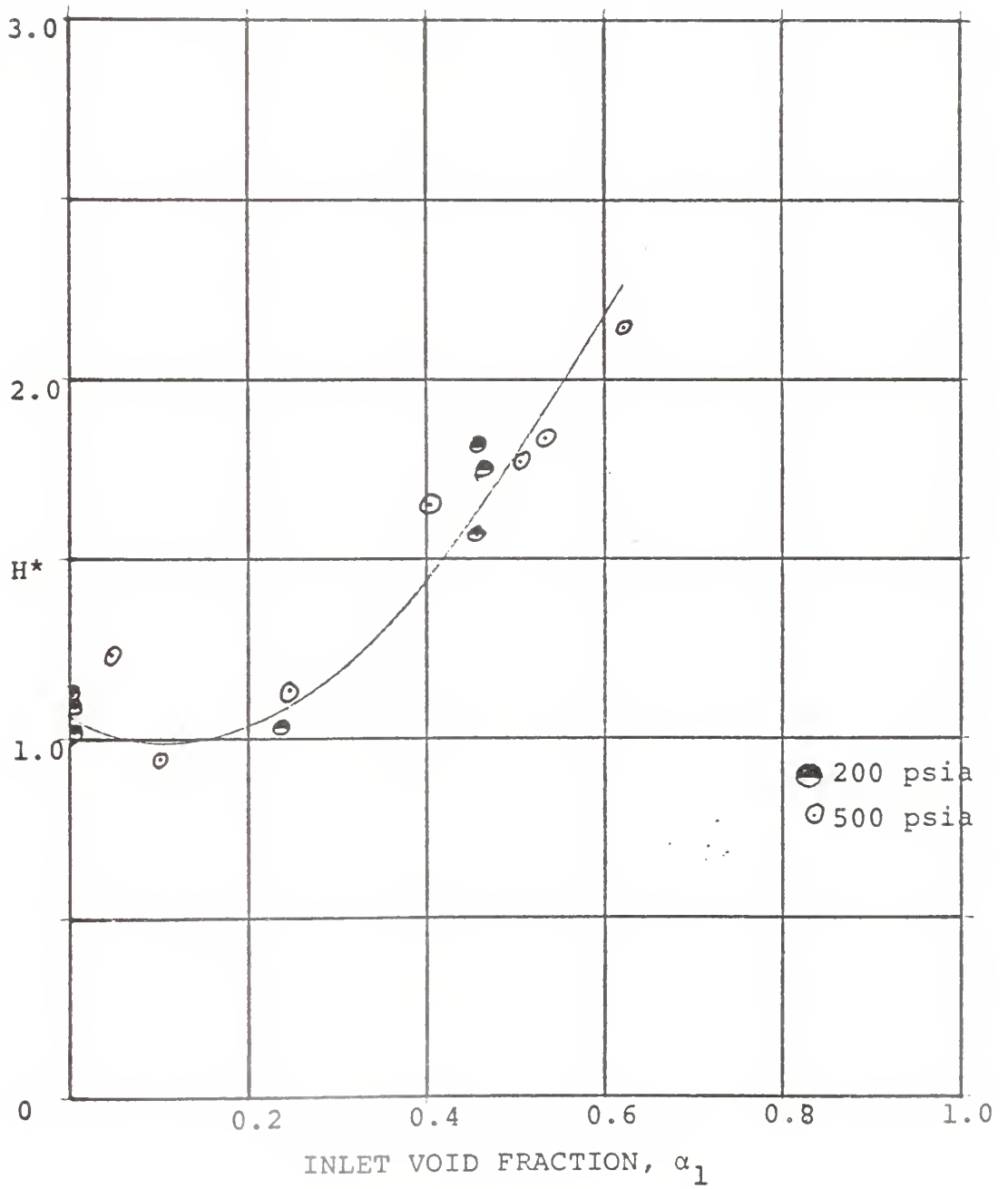

FIGURE E1 - HEAD-LOSS RATIO VERSUS INLET VOID-FRACTION USING EQUATION 9 FOR ψ'_{1thsp}

TABLE E1

CALCULATION OF THE HEAD-LOSS RATIO, H*, USING EXPERIMENTAL DATA TO EVALUATE EQUATION 9

TWO-PHASE TEST NUMBER	$(\psi'_{1thtp})^{\dagger}_{se}$	H*	α_1
150	0.199	1.581	0.461
151	0.006	1.816	0.464
152	-0.092	1.763	0.466
153	-0.102	1.100	0
154	-0.101	1.124	0
155	0.096	1.023	0
156	0.336	1.030	0.241
157	0.341	0.964	0.116
158	0.306	1.142	0.245
159	0.059	1.238	0.056
160	0.189	1.776	0.512
161	0.097	1.835	0.537
162	0.128	2.156	0.631
163	-0.022	1.660	0.401

$$\psi'_{1thtp} = -0.1896 + \left(8.1342\, f_{tpl} + 1.021\, \frac{\rho_{tpl}}{\rho_{tp2}}\, f_{tp2}\right) \phi_{tpl}$$

Values for f_{tpl}, f_{tp2}, ρ_{tpl}, and ρ_{tp2} were obtained from Appendix B.

†where subscript se ≡ semi-empirical

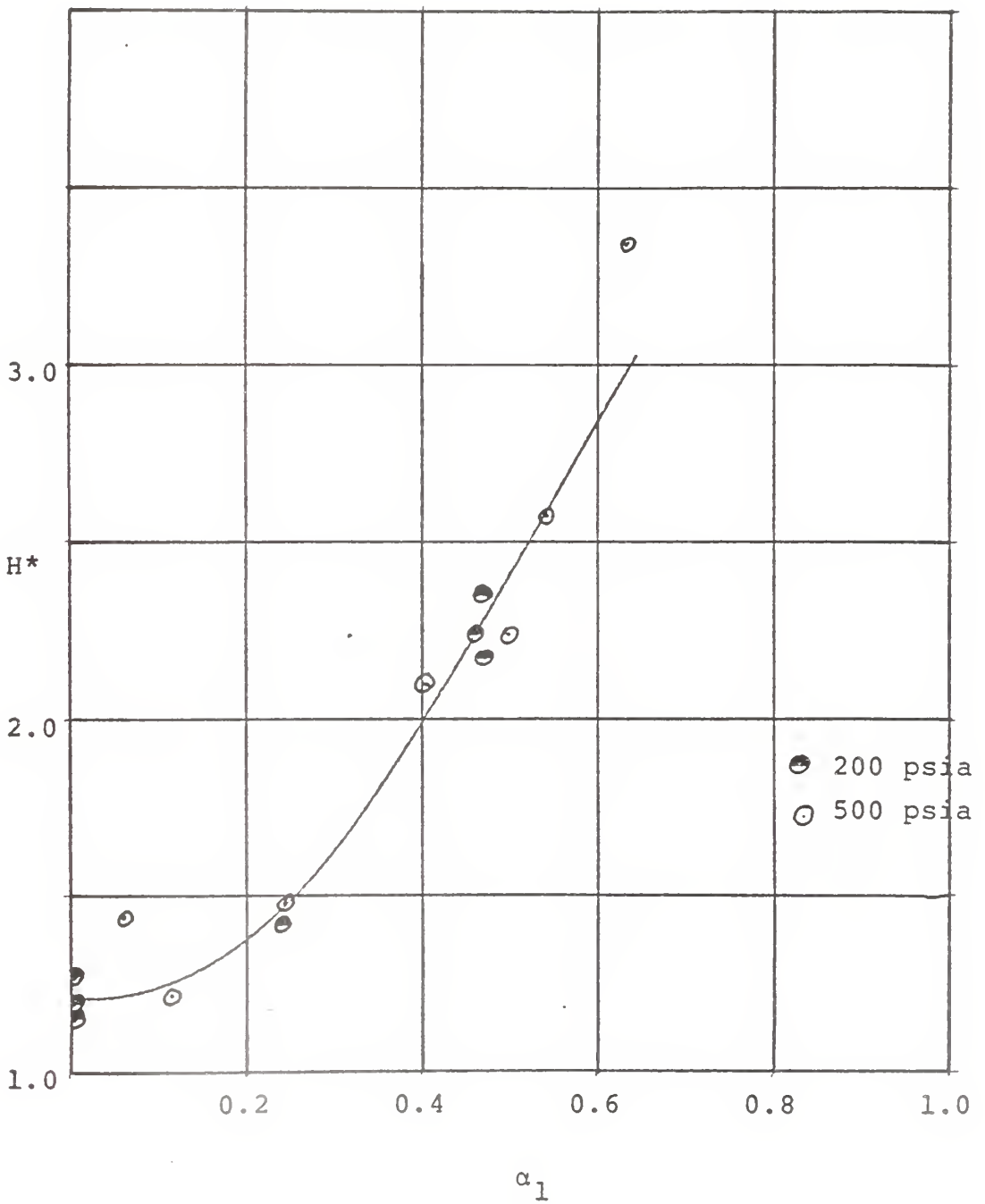

FIGURE E2 - HEAD-LOSS RATIO VERSUS INLET VOID FRACTION FOR ZERO-SWIRL AT OUTLET, $C_{\theta 2} = 0.$

TABLE E2

CALCULATION OF THE HEAD-LOSS RATIO, H*,

ASSUMING ZERO SWIRL AT ROTOR OUTLET, $C_{\theta 2} = 0$

TWO-PHASE TEST NUMBER	ψ'_{lspth}	ψ'_{ltpth}	H*
150	0.248	0.253	2.24
151	0.146	0.148	2.36
152	0.083	0.085	2.18
153	0.078	0.078	1.15
154	0.079	0.079	1.19
155	0.193	0.193	1.27
156	0.354	0.359	1.41
157	0.385	0.388	1.22
158	0.356	0.358	1.48
159	0.206	0.207	1.43
160	0.298	0.318	2.23
161	0.175	0.179	2.58
162	0.122	0.126	3.35
163	0.128	0.130	2.10

REFERENCES

1. Mikielewicz, J. and Wilson, David Gordon, A METHOD OF CORRELATING THE CHARACTERISTICS OF CENTRIFUGAL PUMPS IN TWO-PHASE FLOW, Department of Mechanical Engineering, the Massachusetts Institute of Technology, August, 1975.

2. Thom, J.R.S., PREDICTION OF PRESSURE DROP DURING FORCED CIRCULATION BOILING OF WATER, International Journal of Heat and Mass Transfer, Vol. 7, pp. 709-724, 1964.

3. Kováts, André, DESIGN AND PERFORMANCE OF CENTRIFUGAL AND AXIAL FLOW PUMPS AND COMPRESSORS, The McMillan Co., 1964, pp. 215-229.

4. Kittredge, C.P., CENTRIFUGAL PUMPS USED AS HYDRAULIC TURBINES, Transactions of the ASME, Journal of Basic Engineering, November, 1959, pp. 1-5.

5. Lottes, P.A. and W.S. Flinn, A METHOD OF ANALYSIS OF NATURAL CIRCULATION BOILING SYSTEMS, Nuclear Science and Engineering, Vol. 1, pp. 461-476, 1956.

6. Stepanoff, A.J., CENTRIFUGAL AND AXIAL FLOW PUMPS, 2nd ed., J. Wiley, New York, 1957.

7. Olson, D.J., EXPERIMENT DATA REPORT FOR SINGLE- AND TWO-PHASE STEADY STATE TESTS OF THE 1 - 1/2 - LOOP MOD-1 SEMISCALE SYSTEM PUMP, Aerojet Nuclear Company, Idaho, for the USAEC, Report UC-78, May 1974.

8. LeBoeuf, Raymond, private communication, December 9, 1975. (Lawrence Pumps, Inc., Lawrence, Mass.)

9. ASME Steam Tables, 1967.

10. Griffith, Peter and Wallace, Graham B., TWO-PHASE SLUG FLOW, Transactions of the ASME, Journal of Heat Transfer, August, 1961, pp. 307-320.

11. Addison, Herbert, CENTRIFUGAL AND OTHER ROTODYNAMIC PUMPS, 3rd ed., Chapman and Hall, London, 1966.

12. Knapp, R.T., COMPLETE CHARACTERISTICS OF CENTRIFUGAL PUMPS AND THEIR USE IN THE PREDICTION OF TRANSIENT BEHAVIOR, Transaction of the ASME, Vol. 59, p. 683, November, 1937.

Thesis
G5416 Goldfinch 195473
Prediction of two-
phase performance of
centrifugal pumps.